Spatial dynamics of brain functional domains: A new avenue to study time-varying brain function

A. Iraji[1,*], Z. Fu[1], E. Damarajua[1], A. Belger[2], J.M. Ford[3,4], S. McEwen[5], D.H. Mathalon[3,4], B.A. Mueller[6], G.D. Pearlson[7], S.G. Potkin[8], A. Preda[8], J.A. Turner[9], J.G. Vaidya[10], T.G.M. van Erp[8], and V.D. Calhoun[1,11,*]

[1]*The Mind Research Network, Albuquerque, NM, United USA*
[2]*Department of Psychiatry, University of North Carolina, Chapel Hill, NC, USA*
[3]*Department of Psychiatry, University of California San Francisco, San Francisco, CA, USA*
[4]*San Francisco VA Medical Center, San Francisco, CA, USA*
[5]*Department of Psychiatry and Biobehavioral Sciences, University of California Los Angeles, Los Angeles, CA, USA*
[6]*Department of Psychiatry, University of Minnesota, Minneapolis, MN, USA*
[7]*Yale University, School of Medicine, New Haven, CT, USA*
[8]*Department of Psychiatry and Human Behavior, University of California Irvine, Irvine, CA, USA*
[9]*Department of Psychology, Georgia State University, GA, USA*
[10]*Department of Psychiatry, University of Iowa, IA, USA*
[11]*Department of Electrical and Computer Engineering, University of New Mexico, Albuquerque, NM, USA*

* Correspondence address to:

Armin Iraji, Ph.D.

Postdoctoral fellow, The Mind Research Network

E-mail: armin.iraji@gmail.com

Or

Vince Calhoun, Ph.D.

President & director of Image Analysis and MR Research, Professor of Translational Neuroscience, The Mind Research Network

Distinguished Professor, Departments of Electrical and Computer Engineering (primary), Neurosciences, Computer Science, and Psychiatry, The University of New Mexico

E-mail: vcalhoun@mrn.org

Abstract

The analysis of time-varying connectivity in functional magnetic resonance imaging (fMRI) has become an important part of ongoing neuroscience discussions. The majority of such studies have focused primarily on temporal variations of functional connectivity among fixed regions of interest (ROIs) or networks of the brain. However, the brain reorganizes its activity on both temporal and spatial scales. Thus an approach which captures time-varying characteristics of brain functional organizations is essential to improving our understanding of brain function. Here, we propose an approach that uses blood oxygenation-level dependent (BOLD) signal to capture spatiotemporal variations of the functional domains of the brain. The approach is based on the well-accepted assumption that the brain can be modeled as a hierarchical functional architecture with different levels of granularity, and as we move to lower levels of this architecture, the complexity associated with each element of this hierarchy decreases. In other words, lower levels have less dynamic behavior and higher functional homogeneity, and there is a level at which its elements can be approximated as “functional units”. A functional unit is a pattern of regions with very similar functional activity over time. At the macro-scale, we suggest high-order intrinsic connectivity networks (hICNs) obtained from a high-order spatial independent component analysis (ICA) provide a way to approximate functional units. We consider hICNs to comprise functional domains, elements of a higher level of the brain functional hierarchy which are being investigated in this study. Focusing on time-varying characteristics of functional domains, our approach captures the unique information of each functional domain at every timepoint and has the capacity to examine spatiotemporal variations of the functional domains up to the maximum temporal and spatial resolutions that exist in the data. Here, k-means clustering was deployed to summarize time-varying characteristics of each functional domain into a set of representatives called spatial domain states. Furthermore, the functional connectivity between domains was examined to identify functional modules. Each functional module contains states of functional domains with higher connectivity with each other than with other states. Our proposed approach was further evaluated using a multi-site dataset of resting-state BOLD/fMRI data collected from

160 healthy controls and 149 patients with schizophrenia (SZ). The findings demonstrate that functional domains are spatially fluid over time. Results highlight a negative relationship between the default mode domain and the attention domain in functional module 3. The same pattern exists between the default mode domain and visual, motor, and auditory domains. This is consistent with previous findings showing a negative correlation between the default mode and these domains. The results also revealed distinct differences in the spatial domain states of SZ patients, primarily in the subcortical domain. Importantly, our findings also show that alterations in functional connectivity can occur in the absence of changes in functional activity and vice versa. In short, our approach demonstrates spatially fluid behavior of intra- and inter-domain relationships and highlights a hierarchy of spatial dynamics providing new insight into macro-level functional connectivity in the human brain.

Keywords:

Brain dynamic, functional domains, spatial coupling, spatial domain states, schizophrenia, high-order independent component analysis, intrinsic activity, resting state fMRI

1. Introduction

Neuronal populations interact and compete in the service of information processing at different spatial (from micro to macro) and temporal scales (millisecond to days), which collectively constitute brain function. At the macro-level, studying functional interactions using fMRI (the macro functional connectome) has made important contributions to our knowledge of brain functional systems. For example, examining the functional connectivity across whole brain using univariate and multivariate approaches identifies multiple replicable large-scale brain networks (Calhoun et al., 2008; Guo et al., 2012; Smith et al., 2009; van den Heuvel et al., 2009; Van Dijk et al., 2010; Yeo et al., 2011). Large-scale networks, also known as distributed networks or functional domains, are comprised of a set of spatially distinct and temporally covarying functional units (sub-networks) that putatively orchestrate various brain functions (van den Heuvel and Hulshoff Pol, 2010). The concept of brain networks is now well-

established, and the stability and reproducibility of several of brain networks have been confirmed by multiple independent investigations (Biswal et al., 2010; Buckner et al., 2009; Franco et al., 2009; Guo et al., 2012; Shehzad et al., 2009; Zuo et al., 2010). Brain networks are significantly associated with different physiological and psychological conditions and have been proposed as a promising property to help improve clinical diagnosis and treatment (Arbabshirani et al., 2017; Garrity et al., 2007; Greicius, 2008; Menon, 2011; Seeley et al., 2009; Sorg et al., 2007). A recent point of discussion in this field is capturing time-varying information of the brain (Calhoun et al., 2014; Hutchison et al., 2013; Preti et al., 2017). Considering the dynamic nature of the brain and changes in brain activity over time, the assumption of static brain networks throughout the length of data acquisitions is oversimplified and obscures proper characterization of the brain function. Thus, recent studies focus on capturing time-varying information of the brain instead of extracting the most dominant patterns of brain networks over the course of the data acquisition. Several strategies have been proposed to study time-varying information in BOLD signal. The most commonly used approach is identifying reoccurring temporal coupling among brain regions using sliding-window approaches (Allen et al., 2014; Damaraju et al., 2014; Sakoglu et al., 2010). Taking into account that temporal variations of the brain can be as quick as milliseconds, capturing the dynamic information in BOLD signals to its full potential can be more informative. As a result, recent studies explore the time-varying characteristics up to the maximum frequency existing in the data (Trapp et al., 2018; Vidaurre et al., 2017; Yaesoubi et al., 2018) by avoiding the assumption of a smooth transition between states. One less investigated aspect of time-varying information of the brain is the variations in the spatial coupling of brain functional organizations. In an early work, Kiviniemi et al. used sliding-window ICA and observed spatial variations in the default mode network (Kiviniemi et al., 2011). Fluctuations in spatial couplings were also detected by measuring residual mutual information between spatial components derived from independent vector analysis (Ma et al., 2014). Beyond this there has been little work; in addition neither of these approaches evaluated the possibility of a hierarchy of spatial dynamics. Because the brain reorganizes itself on both spatial and

temporal scales, approaches that capture variations in spatial and temporal coupling of functional organizations are essential to improve our understanding of brain function.

Here, we devise a novel data-driven approach that employs the BOLD signal to capture and characterize spatiotemporal variations of the functional domains of the brain at different scales within the limitations of the analysis/acquisition approach. Evidence from this study supports the view that functional domains are spatially evolving over time. Indeed, at various times the interactions between and within functional domains involves different spatial regions. Results characterize highly reproducible and distinct patterns of activities, called spatial domain states, within each functional domain. Further application of our approach to SZ patients underline its ability to detect alterations in dynamic characteristics of the activity of functional domains promising potential clinical applications of the approach. A key advantage of the approach is its ability to successfully capture spatiotemporal changes of functional domains without applying constraints on the spatial and/or temporal coupling. The approach does not require using sliding window so it can capture the maximum temporal frequency variations which exist in the temporal profile (Yaesoubi et al., 2018). Furthermore, it allows detecting the fluctuations in the spatial coupling up to the maximum spatial resolution existing in the data.

In summary, we introduce an innovative framework to shed new light on time-varying spatial characteristics of brain function. The approach provides the backbone for examining spatiotemporal variations of brain functional domains and the hierarchy of spatial dynamics which can improve our understanding of brain function. Results also show the potential of further exploitation of these time-varying behaviors to be useful for characterizing mental illness.

2. Method:

2.1. Glossary

There have been many terms and jargon used to define the functional architectures of the brain, for example “network”, “circuit”, “module”, “domain”, and “system” have been used to define the same functional structure. At the same time, each term can also refer to different functional structures across studies. For instance, the term “network” has referred to a collection of elements but at different levels from set of anatomically separated regions to a cluster of functionally homogeneous voxels to cell-specific regulatory pathways inside of neurons (Erhardt et al., 2011; Petersen and Sporns, 2015). Networks sometimes even define as a collection of regions without explicit reference to connections among them (Petersen and Sporns, 2015). As described in (Erhardt et al., 2011), the way to avoid confusion is to ensure that all terms are clearly defined, thus here we provide a glossary of key terms used throughout this paper (Figure 1).

High-order intrinsic connectivity network (hICN): A hICN is comprised of set of voxels (pattern of regions) with very similar functional activity over time (high functional homogeneity at macroscale) that can be approximated as one functional unit. In this work, 65 hICNs were detected using high-order ICA.

Functional domain: A functional domain is a formation of functionally linked hICNs. The nine functional domains are visual, somatomotor, auditory, language, frontoparietal, attention, default mode, and subcortical domains. Functional domains are equivalent to so-called large-scale networks or distributed networks. hICNs were assigned to functional domains based on their anatomical and common functional properties that support hICNs relevance to the functional domains.

State of functional domain: The activity patterns of functional domains vary over time due to the dynamic nature of neural activities. Time-varying information of functional domains can be summarized as a set of states using k-means clustering, in which each cluster (i.e. state) includes time points with a similar activity pattern.

Functional module: Time-varying brain behavior/activity occurs at different scales. At global scale, chronnectome (time-varying properties of connectivity) can be captured as changes in temporal coupling between functional domains. States of functional domains that reoccur together more often than with others in a distinguishable manner were designated “functional modules” and estimated using the Newman modularity detection approach.

(a) Brain is a hierarchical functional architecture

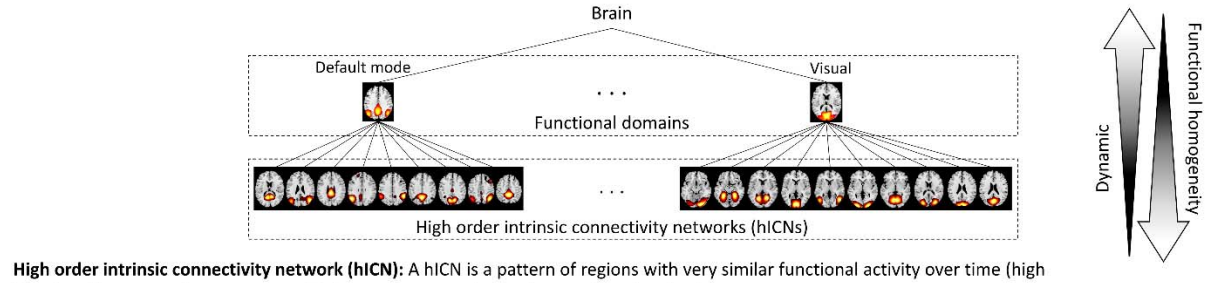

High order intrinsic connectivity network (hICN): A hICN is a pattern of regions with very similar functional activity over time (high functional homogeneity at macroscale) that can be approximated as one functional unit.

Functional domain: A functional domain is a formation of functionally linked hICNs. The nine functional domains are visual, somatomotor, auditory, language, frontoparietal, attention, default mode, and subcortical domains.

(b) The activity of each functional domain varies over time and can be summarized into a set of spatial states

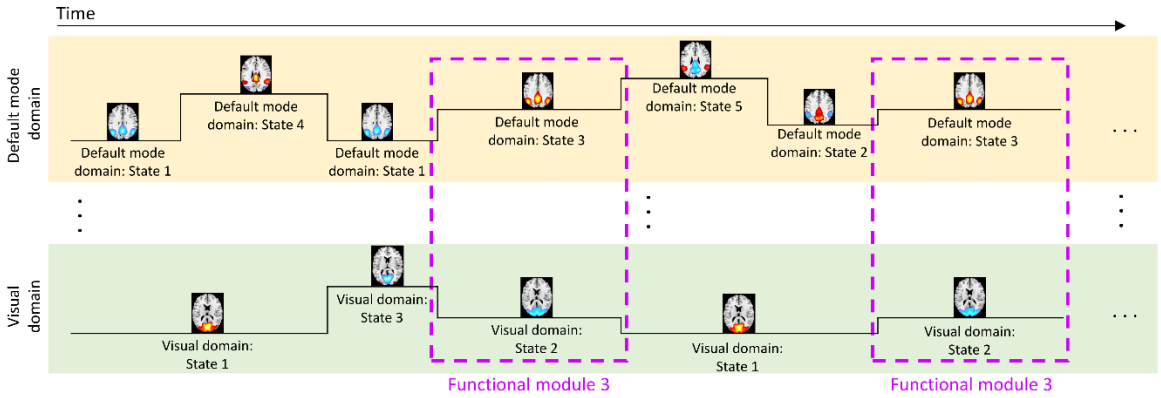

State of functional domain: The activity patterns of functional domains vary over time due to the dynamic nature of neural activity. Time-varying information of each functional domain can be summarized as a set of states using k-means clustering, in which each cluster (i.e. state) includes time points with a similar activity pattern. The definition of functional module in part (c).

(c) Functional module: States of functional domains that reoccur together more often than with others in a distinguishable

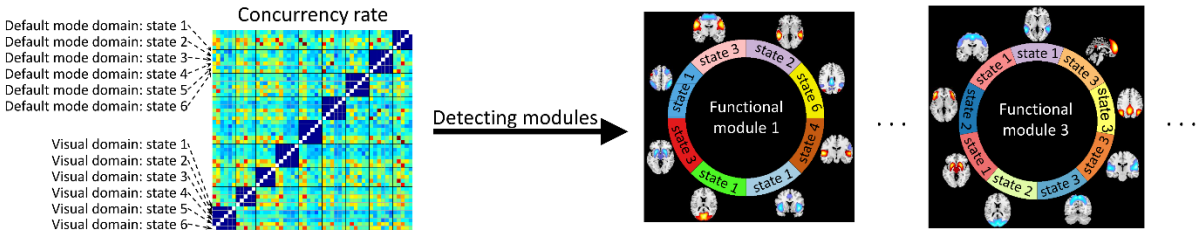

Functional module: Time-varying brain behavior/activity occurs at different scales. At global scale, chronnectome (time-varying properties of connectivity) can be captured as changes in temporal coupling between functional domains. States of functional domains that reoccur together more often than with others in a distinguishable manner were designated "functional modules" and estimated using the Newman modularity detection approach.

Figure 1. Hierarchical functional architectures of the brain and notations used in this work.

2.2. Outline of the approach

The approach includes the following steps. 1) high-order spatial independent component analysis (ICA) is applied to detect the functional units (hICNs) of the functional domains. Using high-order ICA instead of

predefined anatomical locations allows us to detect functionally homogeneous regions from data itself (Calhoun and de Lacy, 2017). 2) hICNs associated with each functional domain are determined through a semi-automatic process. 3) For each individual, the spatial maps and time courses of hICNs are obtained from subject-level spatially-constrained ICA. The time course of each hICN describes the temporal evolution of the hICN. 4) Functional domains, at a given point in time, are reconstructed from the associated hICNs and their time courses at each time point. 5) K-means clustering is applied to summarize the time-varying information of functional domains as a set of spatial states (i.e. cluster), in which each state includes time points with a similar activity pattern. 6) Finally, the Newman modularity detection approach is adopted to study the interaction between functional domains and to detect functional modules.

2.3. Data collection and acquisition parameters

Data collection was performed at 7 imaging sites across United States and passed data quality control. All participants were at least 18 years old and written informed consent was collected prior to enrollment. Data was collected from 160 healthy subjects including 46 females and 114 males (average age: 36.71 ± 10.92; range: 19-60 years) and 149 age- and gender- matched SZ patients including 36 females and 113 males (average age: 37.95 ± 11.47; range: 18-60 years). Further details can be found in our earlier work (Damaraju et al., 2014).

MRI data were collected on a 3-Tesla Siemens Tim Trio scanner for six of the seven sites and on 3-Tesla General Electric Discovery MR750 scanner at one site. Resting state fMRI data was collected using a standard gradient echo EPI sequence with following imaging parameters: pixel spacing size = 3.4375 × 3.4375 mm, FOV of 220 × 220 mm, matrix size = 64 × 64, slice thickness = 4 mm, slice gap = 1 mm, TR/TE = 2000/30 ms, flip angle = 77°, 162 volumes, and Number of excitations (NEX) = 1. During the resting state fMRI scans, participants were instructed to keep their eyes closed and rest quietly without falling asleep.

2.5. Preprocessing

Data were preprocessed using a combination of SPM (http://www.fil.ion.ucl.ac.uk/spm/) and AFNI (https://afni.nimh.nih.gov) software packages including brain extraction, motion correction using the INRIAlign, slice-timing correction using the middle slice as the reference time frame, and despiking using AFNI's 3dDespike. The data of each subject was subsequently registered to a Montreal Neurological Institute (MNI) template and resampled to 3 mm^3 isotropic voxels, and spatial smoothed using a Gaussian kernel with a 6 mm full width at half-maximum (FWHM = 6 mm). Finally, voxel time courses were z-scored (variance normalized) as it has shown improved parcellation of functional organizations structures (hICNs) compared to other scaling methods for independent component analysis.

2.6. High-order intrinsic connectivity network (hICN) extraction

ICA analysis was applied to obtain hICNs. Group ICA analysis was performed using the GIFT software package from MIALAB (http://mialab.mrn.org/software/gift/) (Calhoun and Adali, 2012; Calhoun et al., 2001). First, subject-specific data reduction was performed using spatial principal components analysis (PCA) to retain 95% of the variance of the data of each subject. Next, the retained principal components of subjects were concatenated across time and a group-level spatial PCA was applied. The 200 principal components that explained the maximum variance were selected as the input for a high-order group-level spatial-ICA to calculate 200 group independent components (Figure 2.A). High-order ICA allows us to segment the brain into a set of spatial patterns with very similar functional activity (high functional homogeneity) at macroscale called hICNs. Infomax was chosen as the ICA algorithm because it has been widely used and compares favorability with other algorithms (Correa et al., 2007; Correa et al., 2005). Infomax ICA was repeated 100 times using ICASSO framework (Himberg et al., 2004), and the 'best run' was selected to obtain a stable and reliable estimation (Calhoun and Adali, 2002; Calhoun et al., 2009; Correa et al., 2007; Du et al., 2014; Ma et al., 2011). The independent components associated with the neural activity (hICNs) were selected as those which have peak activations in the gray matter and high spatial similarity with the selected functional domains. Moreover, their time-courses were dominated by

low-frequency fluctuations evaluated using dynamic range and the ratio of low frequency to high frequency power (Allen et al., 2011). Sixty-five cortical and subcortical hICNs were selected and categorized into nine brain functional domains including visual, somatomotor, auditory, language, frontoparietal, attention, default mode, and subcortical domains based on their anatomical and common functional properties (Figure 2.B).

2.7. Functional domain reconstruction

At any given timepoint, functional domains were obtained from the associated hICNs and their contributions as follows. First, subject-specific hICNs and their time courses were calculated via a spatially constrained ICA approach using the group-level hICNs as references (Figure 2.C) (Lin et al., 2010). The time courses of hICNs represent their contributions to the BOLD signal at different timepoints. To reduce noise, we follow a previously published procedure which has proven effective (Damaraju et al., 2014). Two procedures were evaluated for post hoc cleaning: 1) cleaning procedures were applied on the time courses of hICNs, and 2) cleaning procedures were applied on voxel-level after reconstructing the spatial maps of functional domains. The evaluated post-hoc cleaning procedures include 1) orthogonalizing with respect to estimated subject motion parameters, linear detrending, despiking, and band-pass filtering using a fifth-order Butterworth (0.001-0.15 Hz), 2) replacing the Butterworth filter with a Gaussian moving average filter with different window sizes (10×TR to 90×TR) and keeping the rest of cleaning steps the same as the first procedure, 3) using only a Gaussian moving average (with different window size from 10×TR to 90×TR), and 4) no post-hoc cleaning procedure. The various approaches resulted in almost identical spatial dynamic states suggesting that post-hoc cleaning procedures do not substantially alter the dynamic properties of the brain functional domains. Given the similarity of the two approaches, we utilized the first procedure as the computational load was much lower.

After denoising, each function domain was reconstructed using the linear combination of the associated hICNs and their contributions at any given time point resulting in 49749 (309 subjects × 161 timepoints) spatial maps for each functional domain (Figure 2.D and Equation.1).

$$\boldsymbol{FD}_k(t, v) = \sum_{i_k=1}^{N_k} \boldsymbol{w}_{i_k}(t) \times hICN_{i_k}(v) \qquad \text{Equation. 1}$$

Where $\boldsymbol{FD}_k(t, v)$ is the functional domain k at the timepoint t, v is voxel index, N_k is the number of hICNs belongs to the functional domain k, $hICN_{i_k}(v)$ is the hICN #i_k of the functional domain k, and $\boldsymbol{w}_{i_k}(t)$ is the contribution of ICN_{i_k} at the timepoint t.

2.8. Spatial domain states identification using k-means clustering

To evaluate the time-varying information of functional domains, k-means clustering was applied to summarize the spatial maps of each functional domain into a group of spatial patterns called spatial domain states (Figure 2.E). This procedure enables us to acquire representatives describing time-varying behaviors of functional domains and examine the time-varying characteristics of functional domains. The correlation distance metric was used to measure the similarity between data points (i.e. the spatial maps) as it is more sensitive to detect spatial patterns irrespective of voxel intensities. The number of states (clusters) for each functional domain was determined using the elbow criterion by searching for the number of clusters from 3 to 15 (Damaraju et al., 2014; Yaesoubi et al., 2017). In addition, an exploratory analysis demonstrated consistent states for all functional domains over a large range of number of clusters. Similar to what we have done previously (Allen et al., 2014), initial clustering was performed on a subset of the data exhibiting maximal deviation from the mean (called exemplars) and was repeated 100 times with different initializations using k-means++. Exemplars are the data points in which the amount of variance explained by either of hICNs is significantly ($p < 0.001$) higher than the average amount of variance explained by hICNs across whole dataset (49749 fMRI volumes). The estimated centroids from initial clustering using exemplar were then used as cluster center initializations to cluster the whole dataset.

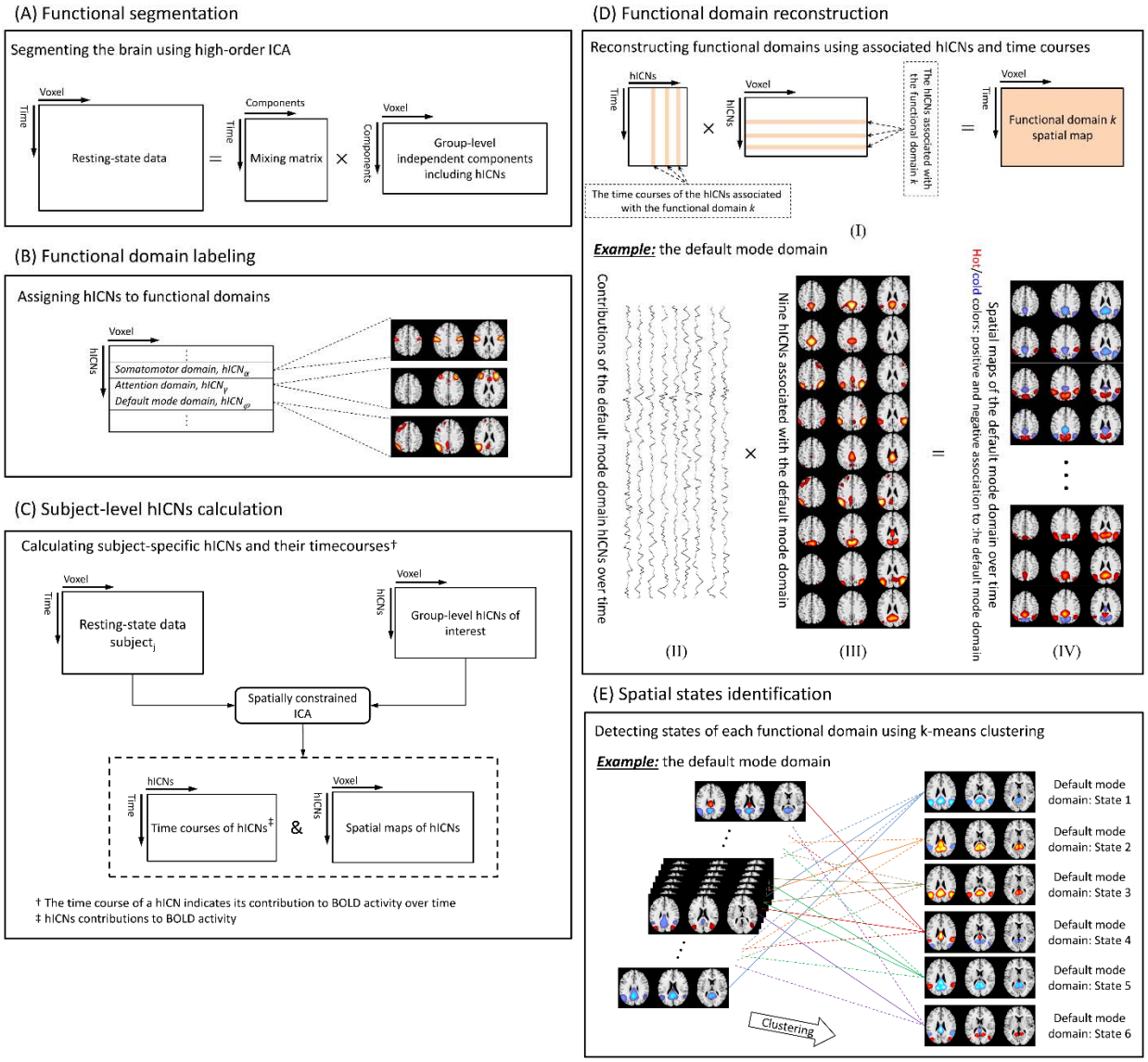

Figure 2. Schematic of the analysis pipeline. (A) High-order group ICA (# Components =200) was applied on the processed resting-state fMRI data from 309 individuals. (B) Sixty-five components were identified as the high-order intrinsic connectivity networks (hICNs) of interests and assigned to one of nine cortical and subcortical functional domains including attention, auditory, default mode, frontal default mode, frontoparietal, language, somatomotor, subcortical, and visual domains (Figure 3). (C) Spatially constrained ICA (Lin et al., 2010) was used to estimate the time courses of hICNs and their spatial maps for each individual. The time course of a hICN indicates the contribution of the hICN at any given time. (D) Functional domains were reconstructed using the linear combination of the associated hICNs and their contributions at any given time. (E) Spatial domain states associated with each functional domain were estimated using k-means clustering on the spatial maps of the functional domain.

2.9. Functional domain variation

To evaluate changes in functional domains over time, we first identified the anatomical regions associated with the states of each functional domain using a brain atlas. A voxel-wise one sample t-test was applied to the data of each state (i.e. the spatial maps of a given functional domain at time points belongs to the spatial domain state), and the average *t*-value was calculated for 246 regions of the Brainnetome atlas (Fan et al., 2016). A region was assigned to a state if its average *t*-value falls outside the Tukey inner Fences (below lower inner fence or above upper fence). A Tukey inner fence is defined as $[Q_1\text{-}1.5\times(Q_3\text{-}Q_1)\ Q_3\text{+}1.5\times(Q_3\text{-}Q_1)]$, where Q_1 and Q_3 are the first and third quartiles (Hoaglin et al., 1986).

Next, we investigated the overall variations in functional domains by calculating changes in regions' participations to functional domains across states. Previously, Cole et al. developed an index called the "global variability coefficient (GVC)" to evaluate variations in the connectivity of the brain networks across different tasks using multi-task fMRI data (Cole et al., 2013). Their results show changes in the connectivity patterns of networks with the frontoparietal and subcortical networks have the highest and the lowest variations, respectively (see Figure 4 of (Cole et al., 2013)). We introduce a related measure called the variability index (VI) to evaluate the level of variability for each functional domain. Similar to GVC, VI is defined as the standard deviation of a region's association to a functional domain which can be estimated using the standard deviation equation of binomial distribution. For example, if functional domain *i* has 5 states, and region *j* is involved in only one state, the standard deviation of the region *j* being associated with the functional domain *i* is $(5 \times 0.2 \times 0.8)^{0.5}$. The average of VI can be used to summarize the overall variability of each function domain.

2.10. Statistical analysis

The approach was evaluated in the context of comparing group differences between the spatial domain states of functional domains estimated from patients with schizophrenia and healthy controls. For each region associated with a given spatial domain state, the average value of the functional domain was

compared between two groups using a general linear model (GLM) that included age, gender, site, and a mean framewise displacement (meanFD) as covariates. meanFD was added as a covariate to mitigate against effects of motion (Power et al., 2012). Statistical results were corrected for corrected for multiple comparisons using the false discovery rate (FDR) (Benjamini and Hochberg, 1995).

2.11. Functional state connectivity and functional modules

Brain functional domains, like other structures of this hierarchical functional architecture, interact with each other. This interaction can be evaluated by calculating the pair-wise functional connectivity between functional domains. Functional connectivity is defined as the temporal dependency of neural activity (Friston et al., 1993). In fMRI, functional connectivity is typically measured by calculating the temporal coherence between BOLD time series or time series associated with brain networks. Using the same strategy, we can estimate functional connectivity between functional domains by calculating the temporal coherence (coupling) between states of functional domains. For this purpose, we calculate the level of concurrency between pairs of states using a coincidence index known as the Dice similarity coefficient (DSC) (Dice, 1945). The functional connectivity between state *i* of functional domain *m* ($FD_{m,i}$) and state *j* of functional domain *n* ($FD_{n,j}$) was calculated as the ratio of the number of the time points that state *i* of functional domain *m* and state *j* of functional domain *n* occurred simultaneously to the average occurrence of state *i* of functional domain *m* and state *j* of functional domain *n* (Equation 2). This we call functional inter-domain state connectivity.

$$Inter-domain\ state\ connectivity\left(FD_{m,i}, FD_{n,j}\right) = DSC\left(FD_{m,i}, FD_{n,j}\right) = \frac{2\times\left|FD_{m,i}\cap FD_{n,j}\right|}{\left|FD_{m,i}\right|+\left|FD_{n,j}\right|} \qquad \text{Equation. 2}$$

We further used functional inter-domain state connectivity values to identify groups of strongly connected states called functional modules. A functional module is defined as a set of states that reoccur together frequently in a distinguishable manner. In other words, a set of spatial domain states with higher connectivity with each other than with other states. Functional modules can be extracted using graph-

based community detection approaches like the Newman modularity detection approach (Newman, 2006). Statistical comparison was further performed on functional modules by comparing each pair of functional inter-domain state connectivity between patients with schizophrenia and healthy controls using the same procedure explained in section 2.10. Statistical analysis.

3. Results

3.1. High-order intrinsic connectivity network (hICN) extraction

Nine cortical and subcortical functional domains were chosen as the domains of interest including attention, auditory, default mode, frontal default mode, frontoparietal, language, somatomotor, subcortical, and visual domains. Among 200 independent components, sixty-five of them were assigned to one of nine functional domains based on the anatomical information and prior knowledge from previous studies (Allen et al., 2011; Ma et al., 2014; Seeley et al., 2009; Yarkoni et al., 2011). We also confirmed the hICN assignment by evaluating the relationship between hICNs and large-scale brain networks obtained from low-order ICA. Figure 3 displays the composite view of the hICNs for each functional domain of interest. The detail information of hICNs including spatial map, coordinates of peak activations, and temporal information can be found in supplementary 1. The selected hICNs are mainly in cortical and subcortical gray matter and show high spatial similarity with hICNs previously identified using high-order ICA (Allen et al., 2011; Damaraju et al., 2014).

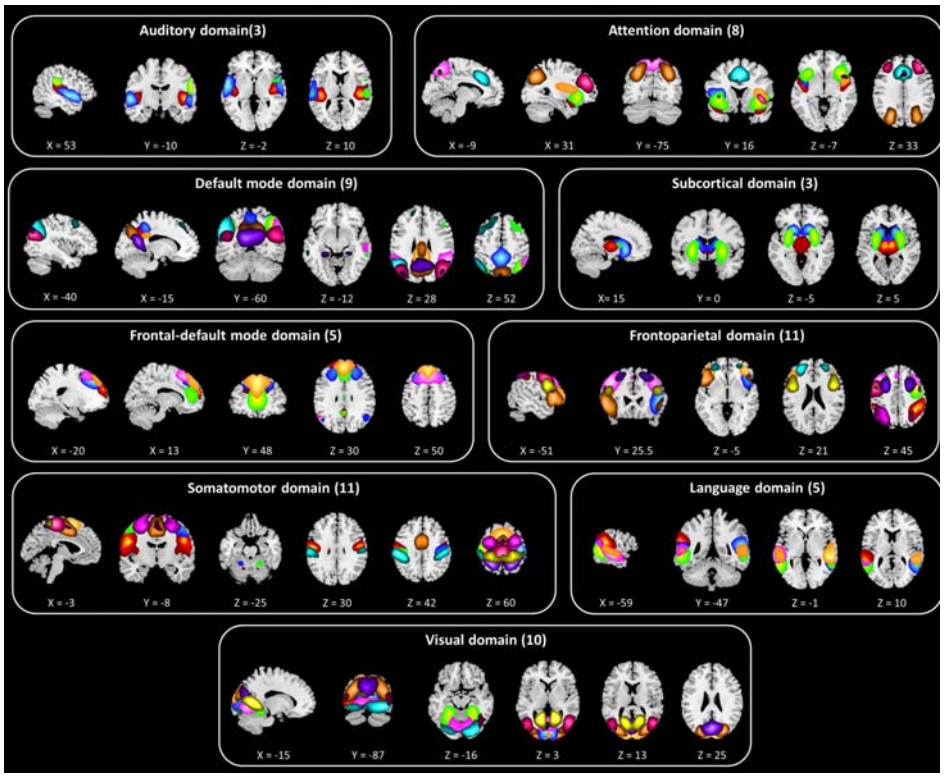

Figure 3. Composite maps of nine functional domains generated from the sixty-five high-order intrinsic connectivity networks (hICNs). Each color in a composite map corresponds to one of hICNs associated with the functional domain. The detail information of hICNs can be found at supplementary 1.

After selecting hICNs of interest, spatially constrained ICA was utilized to calculate the subject-specific hICNs and their time courses (Figure 2.C) which were further used to reconstruct the functional domains for each individual and timepoint.

3.2. Functional domain reconstruction

At each time point, the functional domains were reconstructed using the associated hICNs and their contributions at that time point which results in 49749 (309 subjects × 161 timepoints) spatial maps for each functional domain. Figure 2.D illustrates an example of functional domain reconstruction for the default mode domain which contains nine hICNs shown in Figure 2.D(III). At each timepoint, the default mode domain (Figure 2.D(IV)) was calculated using the linear combination of the nine hICNs, and their contributions (Figure 2.D(I)). In Figure 2.D(IV), hot and cold colors represent positive and negative associations to the default mode domain. The spatial maps of functional domains and their variations over

time for randomly selected individuals are provided as supplementary movies 1–9 and also at the following link https://www.youtube.com/playlist?list=PLZZPPK0O_qFuil41n4U_HSZ668cFDuG7l.

3.3. Spatial domain state identification

Previous studies have demonstrated time-varying connectivity in fMRI data (Allen et al., 2014; Calhoun et al., 2014). As it can be seen in movies 1-9, a similar time-varying phenomenon can be seeing in the spatial properties of functional domains. The functional domains are highly dynamic, and the contributions of brain regions to functional domains vary significantly over time. Brain regions show both strong positive and strong negative associations to functional domains over time. Moreover, as will be demonstrated later in section "3.5. Functional domain variations", the variation in the association of regions to functional domains goes beyond amplitude modulation. For example, some brain regions which are strongly involved in functional domains at a given timepoint become dissociated at other timepoints. To study the time-varying characteristics of functional domains, k-means clustering was applied on the spatial maps of each functional domain and summarized them into a set of reoccurring activity patterns called spatial domain states (Figure 2.E, and for more details, see section 2.7.). The states associated with nine functional domains are illustrated in Figure 4. Spatial maps in Figure 4 represent the centroids of the clusters and reflect the activity patterns (states) present within the clusters. It worth mentioning that the number of clusters (k) was determined using the elbow criterion; however, additional exploratory analyses demonstrate that these clusters are fully reproducible over a large range of k, and activity patterns are very similar across a large range of k (see supplementary 2). In general, we can categorize the states into voxel-wise coherent and incoherent states. In voxel-wise coherent states, the regions associated with functional domains show a similar pattern of association, either positive or negative, while voxel-wise incoherent states contain regions with both positive and negative associations to functional domains. In Figure 4, the total number and percentage of states occurrences are listed above each centroid. Occurrence rates range from 10% to 25%. For all functional domains, the top two dominate states are voxel-wise coherent states with occurrence rates above 20%.

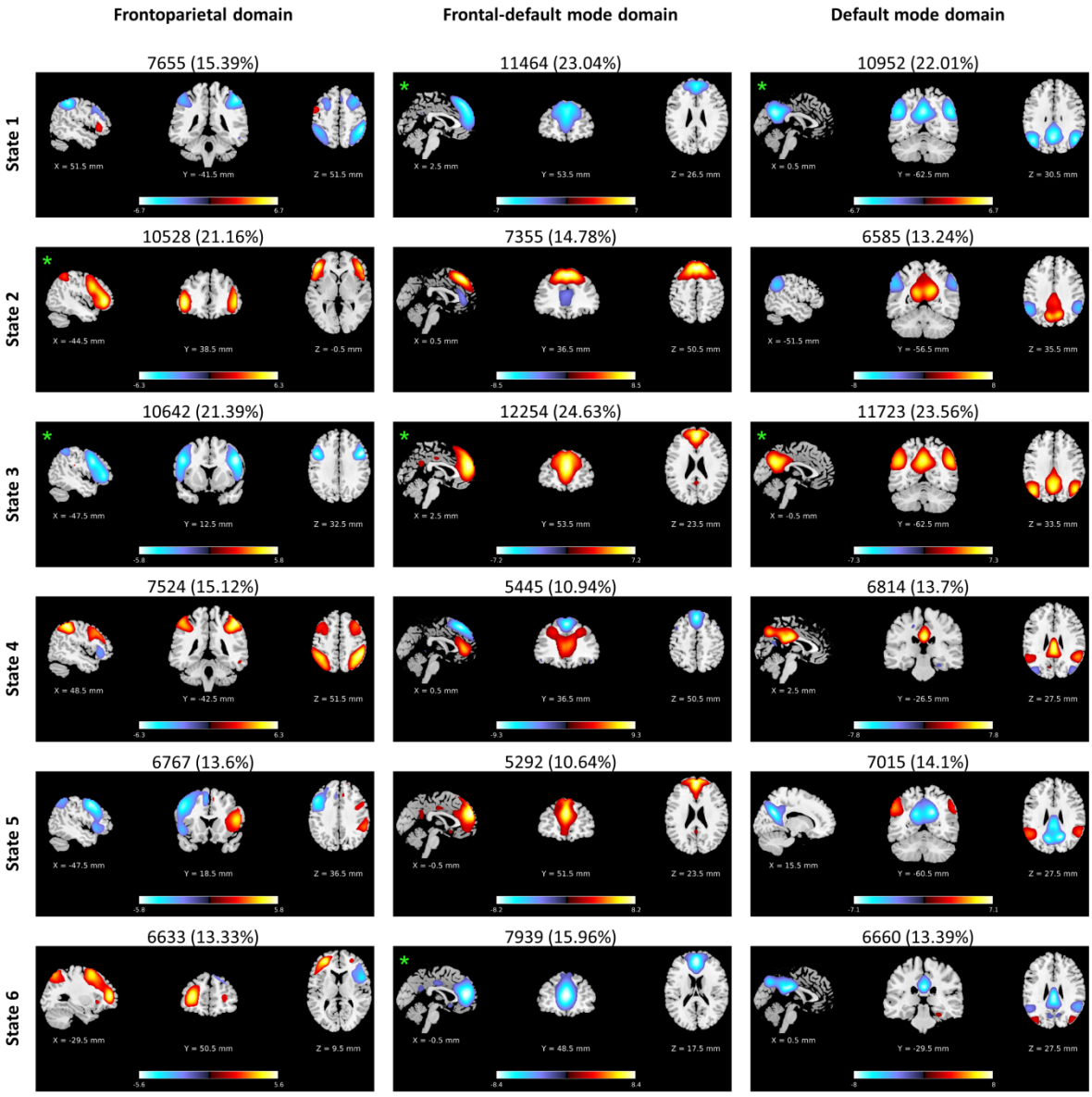

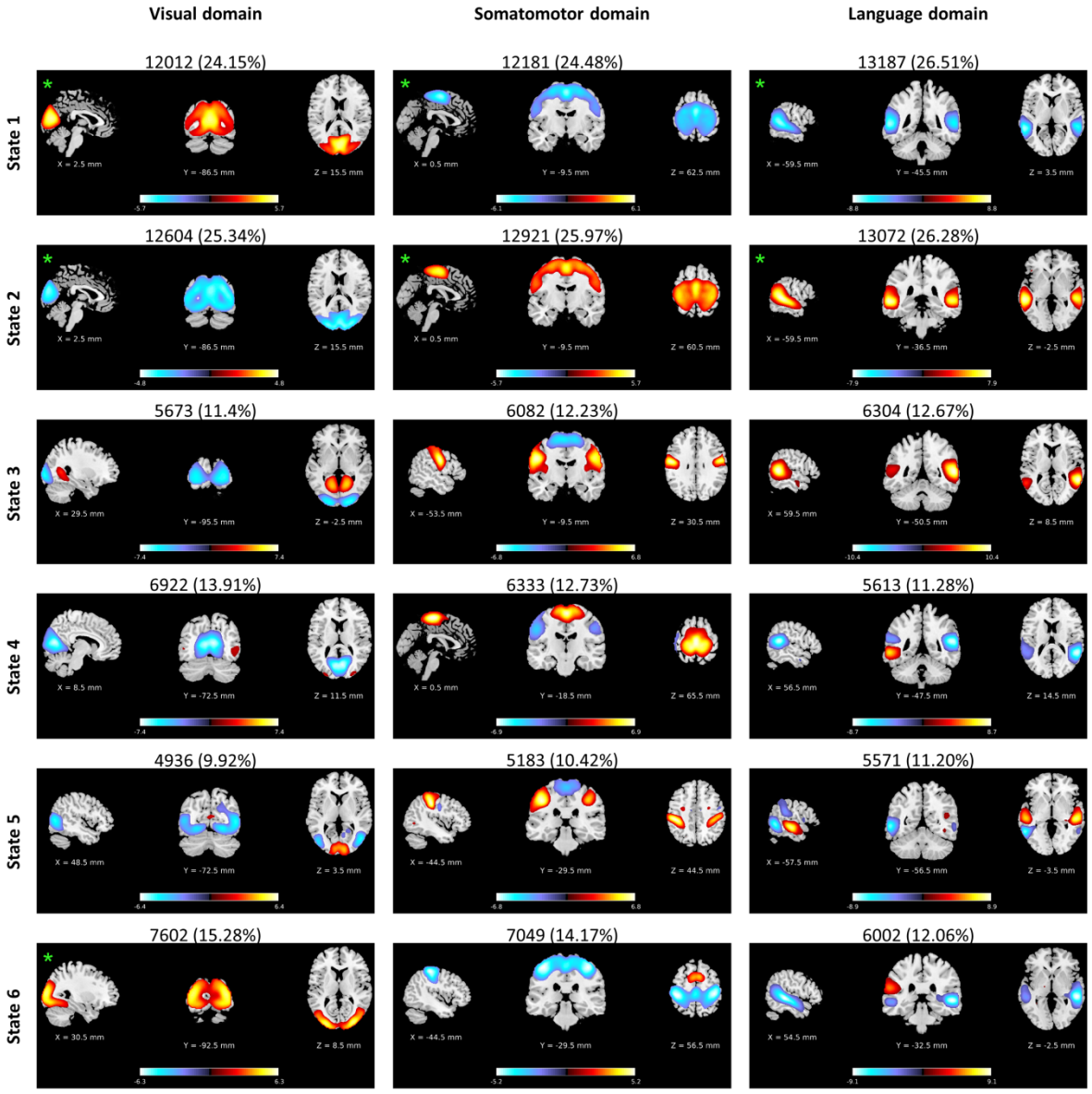

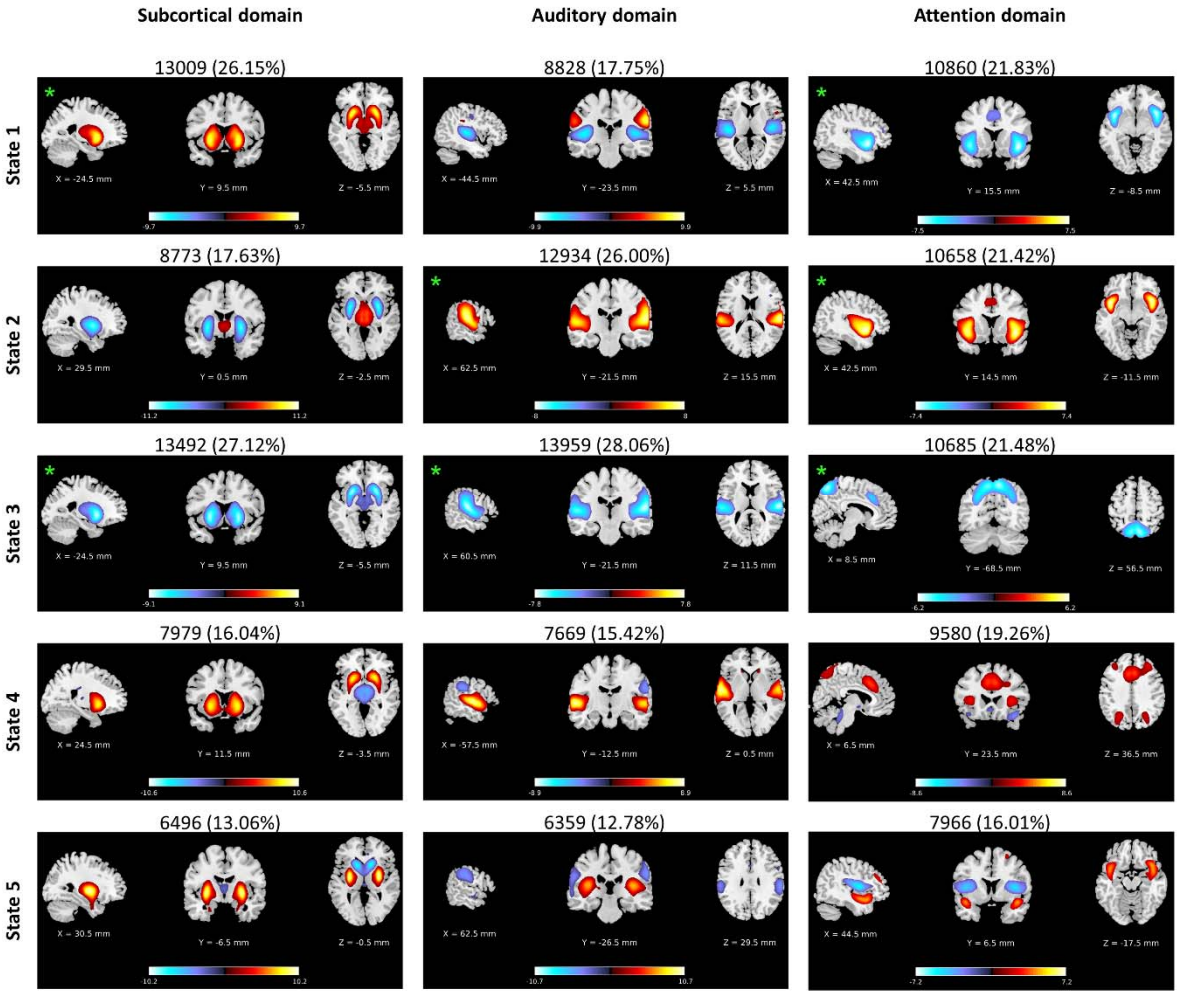

Figure 4. The orthogonal view of the spatial domain states associated with nine functional domains thresholded at $|Z| > 1.96$ ($p = 0.05$). Each spatial map represents the centroid of a cluster, and sagittal, coronal, and axial slices are shown at the peak activation of the centroids. Hot and cold colors represent positive and negative association of voxels to the functional domains. The total number and percentage of occurrences are listed above each centroid. Voxel-wise coherent states were marked using green asterisks. In voxel-wise coherent states, the associated regions show a similar pattern of association, either positive or negative, and voxel-wise incoherent states contain both regions with positive and negative associations to functional domains. It worth mentioning that because the orthogonal view represents the peak activations of the centroids, we cannot see both positive and negative contributions for voxel-wise incoherent states for some cases including the state 5 of the frontal default mode domain and state 3 of the language domain. For further details of regions associations please see Figure 6.

3.4. BOLD response across states (validation)

We further verified our findings by evaluating the average BOLD signal of associated regions across states. Let us assume region *j* is only associated with functional domain *k*. Then, if the association of region *j* to functional domain *k* is positive/negative at state *i*, the neural activity of region *j* measured by

the BOLD signal at the state *i* of functional domain *k* should be above/below its average (i.e. the average BOLD signal of region *j*). We expect to observe the same pattern even if regions are associated to different functional domains at the same time. Investigating the relationships between BOLD signal of regions and their contributions to functional domains exhibits overall the same pattern that regions have higher/lower activity when they have positive/negative association to their corresponding functional domains. We observe this agreement between BOLD signals and regions associations to functional domains for 96.02% of the cases. An example of the relationship between BOLD signal and regional association is presented in Figure 5. Further investigation determined that different directionality between regions associations to functional domains and the amplitude of their BOLD signals only occurs in those regions with weak contribution to the functional domains and/or small BOLD signal difference from the baseline (see supplementary 3).

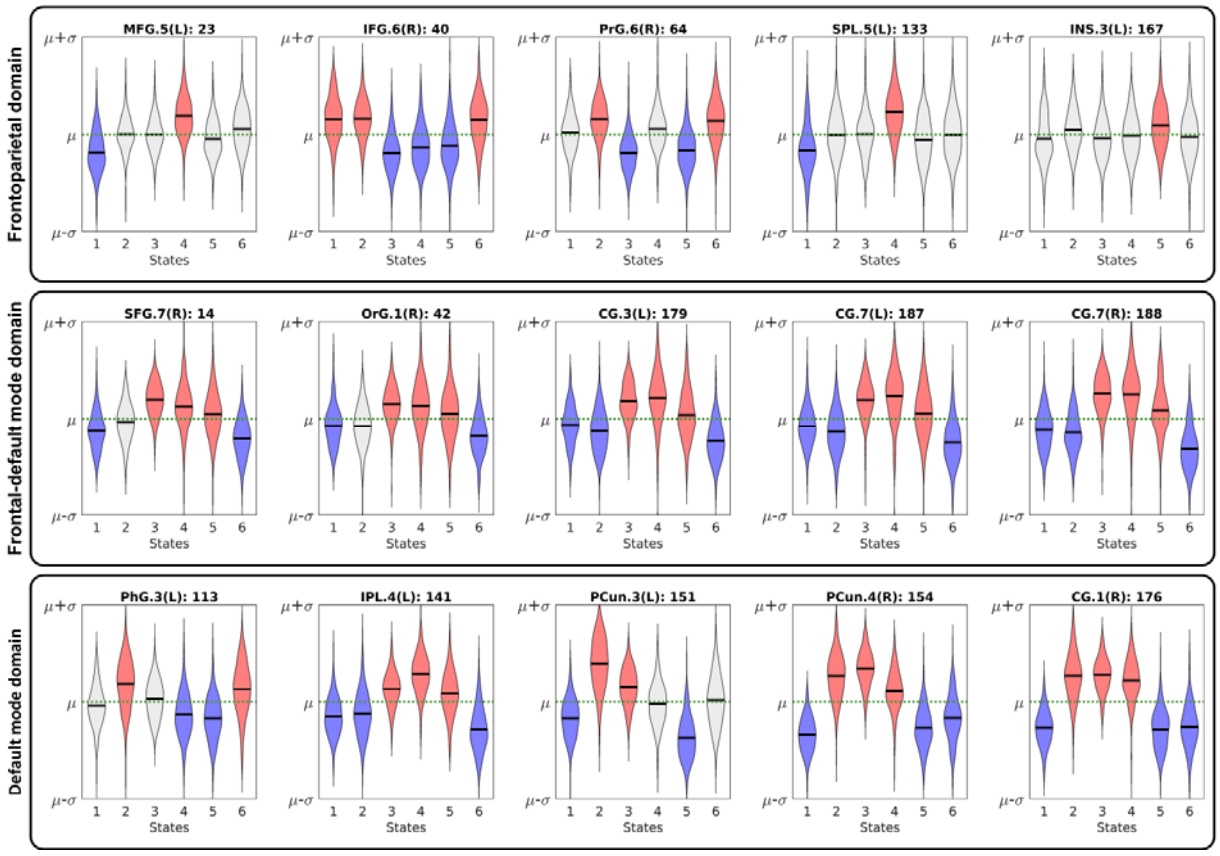

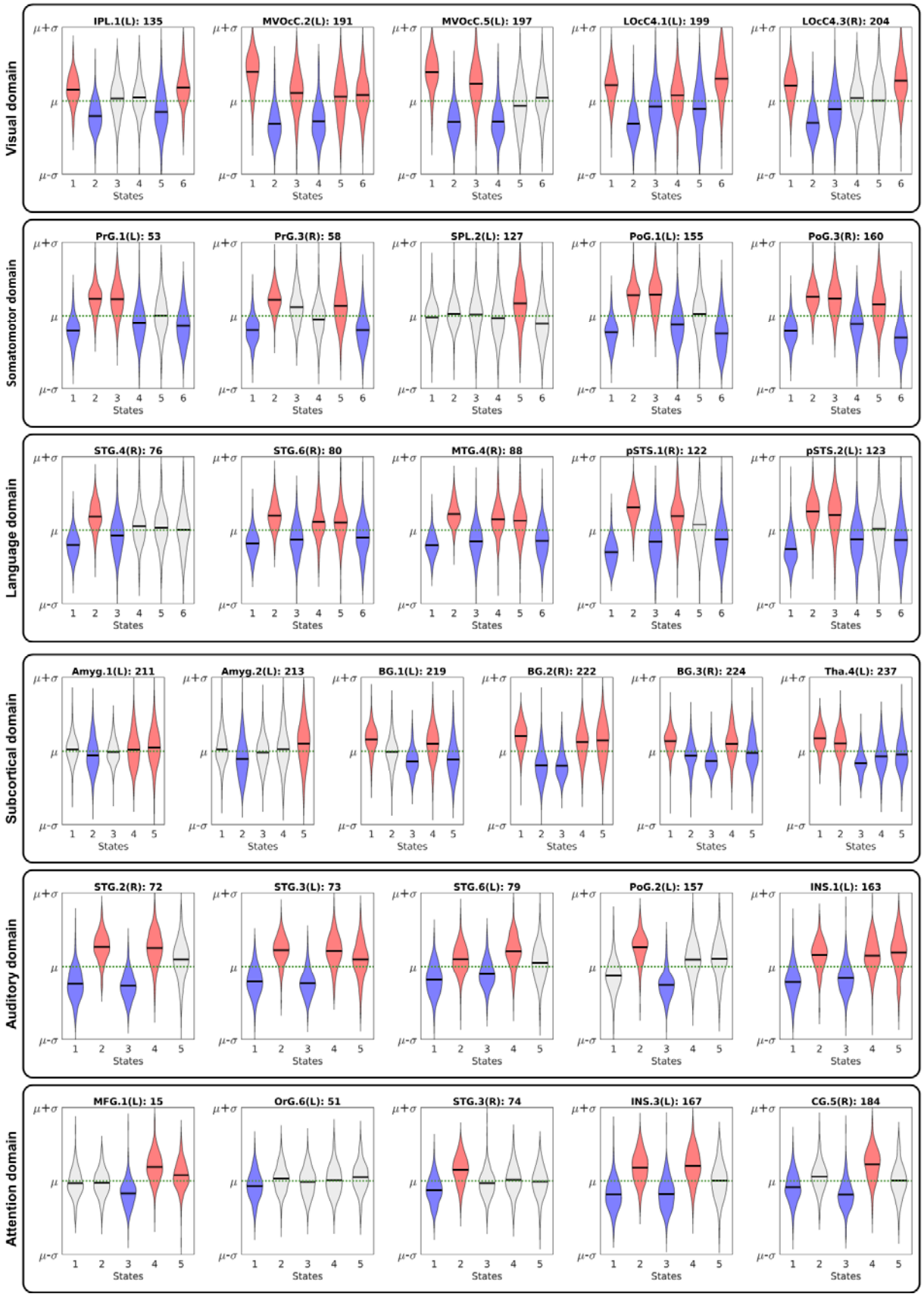

Figure 5. Average BOLD signal of regions across states. Each violin plot represents the average BOLD signal of a region for different states of a functional domain. The μ (green dashed line) and σ are the average and standard deviation of BOLD signal for each region across all time points, and the black line represents the average of the BOLD signal of a region across all subjects in the corresponding state. Red and blue colors represent the states with positive and negative associations of regions to functional domains, the light gray color indicates no association between corresponding functional domain and region. The results show that when regions are positively/negatively associated with functional domains, their average BOLD signal is above/below its own average across all timepoint. This suggests the variation in a region association to a functional domain is related to its neural activity observed by the amplitude of BOLD signal. The total number and percentage of occurrences are listed above each centroid. The abbreviation and regions labels listed above each violin plot are based on the Brainnetome atlas. Amyg (Amygdala), BG (Basal Ganglia), CG (Cingulate Gyrus), IFG (Inferior Frontal Gyrus), INS (Insular Gyrus), IPL (Inferior Parietal Lobule), LOcC (lateral Occipital Cortex), MFG (Middle Frontal Gyrus), MTG (Middle Temporal Gyrus), MVOcC (MedioVentral Occipital Cortex), OrG (Orbital Gyrus), PCun (Precuneus), PhG (Parahippocampal Gyrus), PoG (Postcentral Gyrus), PrG (Precentral Gyrus), pSTS (posterior Superior Temporal Sulcus), SFG (Superior Frontal Gyrus), SPL (Superior Parietal Lobule), STG (Superior Temporal Gyrus), and Tha (Thalamus).

3.5. Functional domain variations

Next, we evaluated the time-varying characteristics of the functional domains. Focusing on regions associated with the functional domains, we observe changes in regions' membership and the strength of their association to functional domains over time. Figure 6 shows regions associated with the functional domains in different states. Hot and cold colors represent positive and negative association, and *t*-value indicates the strength of the regions association to functional domains. The gray arrays indicate dissociation between the regions and functional domains at corresponding states. In other words, if region *j* is not involved in functional domain *k* at the state *i*, the array (*i*,*j*) for functional domain *k* is gray. The list of associated regions, their coordinates, and the strengths of their associations to functional domains can be found at supplementary 4. Our analysis demonstrates distinct patterns for functional domains across states with each involves in different brain regions. This could potentially explain the variability that has been observed in associated regions to different functional domains (large-scale networks) in previous studies. Using multi-task fMRI data and predefined anatomical regions, Cole et al. demonstrated variations in the functional connectivity pattern of the frontoparietal network (Cole et al., 2013). Braga and Buckner observed different patterns for the default mode, frontoparietal, and (dorsal) attention within the individual (Braga and Buckner, 2017). For instance, they observed two district patterns for the default

mode. One includes the parahippocampal cortex and posterior inferior parietal lobule, and the other includes anterior inferior parietal lobule regions. Similar patterns were observed in our work. We found variations in the parahippocampal gyrus and inferior parietal lobule along with many other regions across default mode states. Our finding suggests that the variations observed in the patterns of functional domains could be the results of dynamic variations of regions contributions to functional domains that are obscured when functional domains are obtained using full dataset.

Comparing overall variability of functional domains using a variability index (VI) reveals that the distributed functional domains such as the frontoparietal and attention which are engaged in a wide variety of cognitive functions involve in higher variations than other functional domains. The mean and standard error of VI are listed above the chart of each functional domain in Figure 6. The findings are consistent with previous results using multi-task fMRI data (Cole et al., 2013) in which frontoparietal, attention and auditory, in order, show the highest variation, and the subcortical has the lowest changes in its connectivity pattern (Cole et al., 2013).

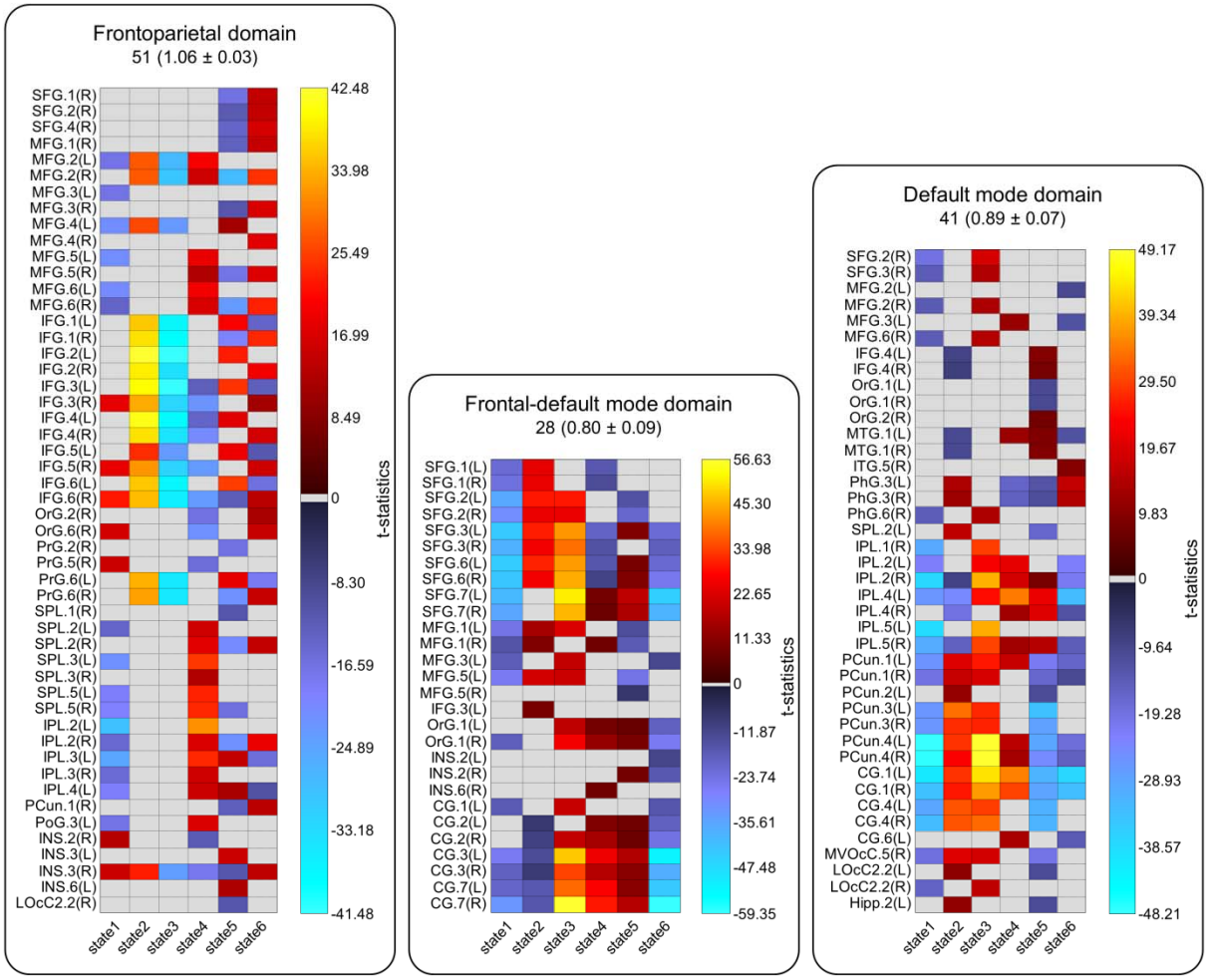

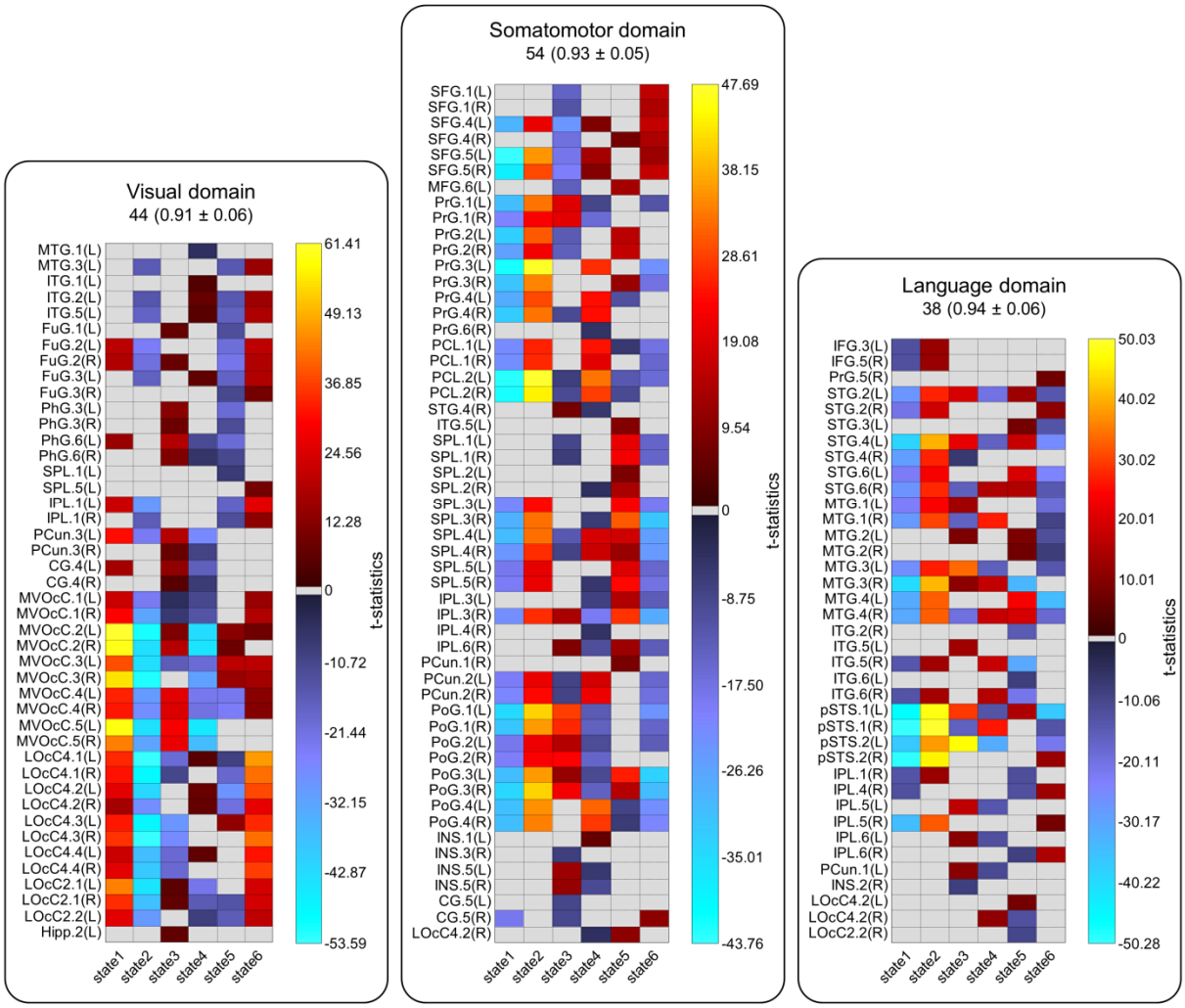

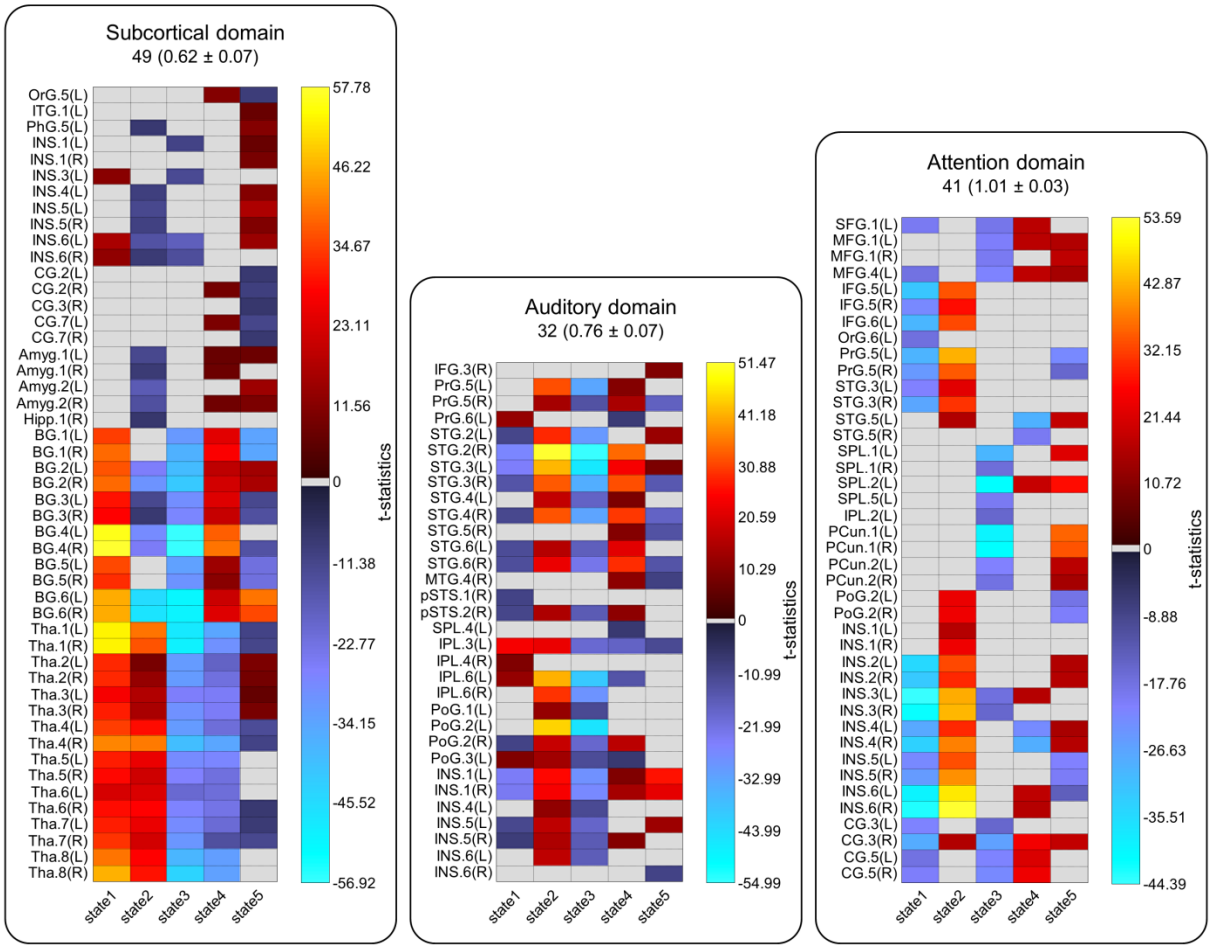

Figure 6. Functional domain variations. Each chart represents the regions associations to a functional domain. The brain anatomical parcellation is based on the Brainnetome atlas. The total number associated regions and the mean and standard error of variability index (VI) are listed above each chart. The results show different regions are associated to functional domains at different states. Hot and cold colors represent positive and negative associations and gray represents dissociation of the regions at the states. VIs represent the overall variability of each function domain where frontoparietal and subcortical domains shows maximum and minimum variations as it was previously observed a multi-task fMRI study (Cole et al., 2013). The abbreviation and regions labels are the same as defined in the Brainnetome atlas. SFG (Superior Frontal Gyrus), MFG (Middle Frontal Gyrus), IFG (Inferior Frontal Gyrus), OrG (Orbital Gyrus), PrG (Precentral Gyrus), PCL(Paracentral Lobule), STG (Superior Temporal Gyrus), MTG (Middle Temporal Gyrus), ITG (Inferior Temporal Gyrus), FuG (Fusiform Gyrus), PhG (Parahippocampal Gyrus), pSTS (posterior Superior Temporal Sulcus), SPL (Superior Parietal Lobule), IPL (Inferior Parietal Lobule), PCun (Precuneus), PoG (Postcentral Gyrus), INS (Insular Gyrus), CG (Cingulate Gyrus), MVOcC (MedioVentral Occipital Cortex), LOcC (lateral Occipital Cortex), Amyg (Amygdala), Hipp (Hippocampus), BG (Basal Ganglia), Tha (Thalamus).

3.6. Group differences in spatial domain states

Differences in functional domains between individuals with schizophrenia and healthy controls were evaluated using a regression model including age, site, gender, and meanFD as covariates. Several functional domains had significantly weaker strength of activity across different states in SZ patients compared to healthy subjects. These results are consistent with previous findings that observed hypoconnectivity within the thalamus and sensory domains (Damaraju et al., 2014). Among all functional domains, the visual, subcortical and attention domains are most affected. For the visual domains, all states except state 5 show significant differences between two groups. The most affected regions in the visual domain include the medioventral occipital cortex, the lateral occipital cortex, and the medioventral of the fusiform gyrus. In the subcortical domain, the thalamus showed significant differences in states 1, 2, and 3. For the attention domain, the left insula and the opercular area of the left Brodmann area (BA) 44 in states 1 and 2, and the lateral area of BA 38 in state 4 show the highest differences. It is worth mentioning that the dorsolateral of BA 37 in state 5 of the language domain is the only comparison that shows a significant increase in its association (higher negative association with the language domain) in SZ patients compared to the healthy controls. The other regions with significant differences in the language domain including right BA 41/42 and the rostral area of left BA 22 demonstrated decreased associations in SZ patients similar to the general pattern. We also performed further exploratory analysis on a subsample of the data with little head motion and no significant difference in meanFD between two groups (p-value = 0.5) and observed a similar pattern in group difference as using the full dataset. The full details of spatial comparison and regions with statistical differences can be found in supplementary 5.

3.7. Functional state connectivity and functional modules

The functional state connectivity matrix was estimated by calculating the temporal coupling between the states of functional domains using DSC index (Figure 7). Using the Newman modularity detection approach, seven functional modules were detected (Figure 8). Investigating group differences reveals an overall decrease in functional inter-domain state connectivity within functional modules in SZ patients

showing as the green lines in Figure 8. The group difference is the most pronounced in functional module 1 which mainly includes hypoconnectivity between the subcortical and others domains (Figure 8). Hypoconnectivity of the subcortical domain which is also observed in other functional modules is the largest patient/control differences between groups. Note that the subcortical domain demonstrates alterations in both its activity patterns and its connectivity with other functional domains in states 1, 2, and 3 which were the major source of the observed hypofunction in schizophrenia. Alteration in functional state connectivity of the default mode within functional modules is another interesting finding. Although the comparisons of the spatial domain states of the default mode between two groups did not reveal any significant difference (3.6. Group differences in spatial domain states), hypoconnectivity between the default mode and several functional domains was observed within functional modules. Interestingly, we observed hypoconnectivity between state 2 of the default mode domain and state 5 of the auditory domain while neither of them shows significant change in their activity patterns in SZ patients. This suggests that alterations in functional connectivity can occur in the absence of changes in functional activity and vice versa.

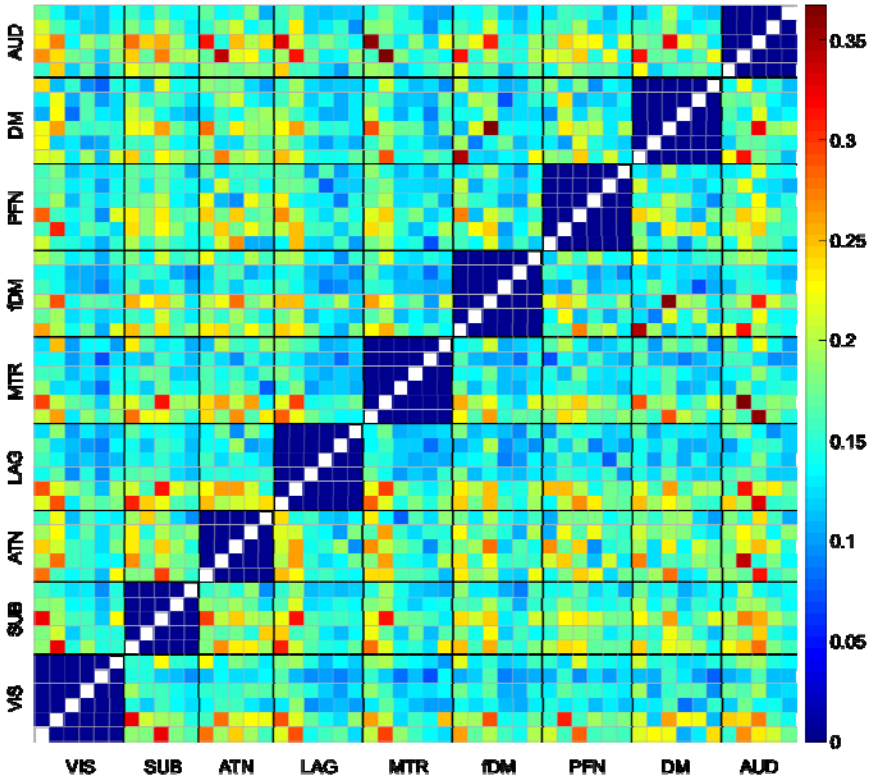

Figure 7. Functional state connectivity was estimated by calculating the level of concurrency between spatial domain states using DSC index. VIS (visual domain), SUB (subcortical domain), ATN (attention domain), LAG (language domain), MTR (somatomotor domain), fMD (frontal default mode domain), PFN (frontoparietal domain), DM (default mode domain), and AUD (auditory domain).

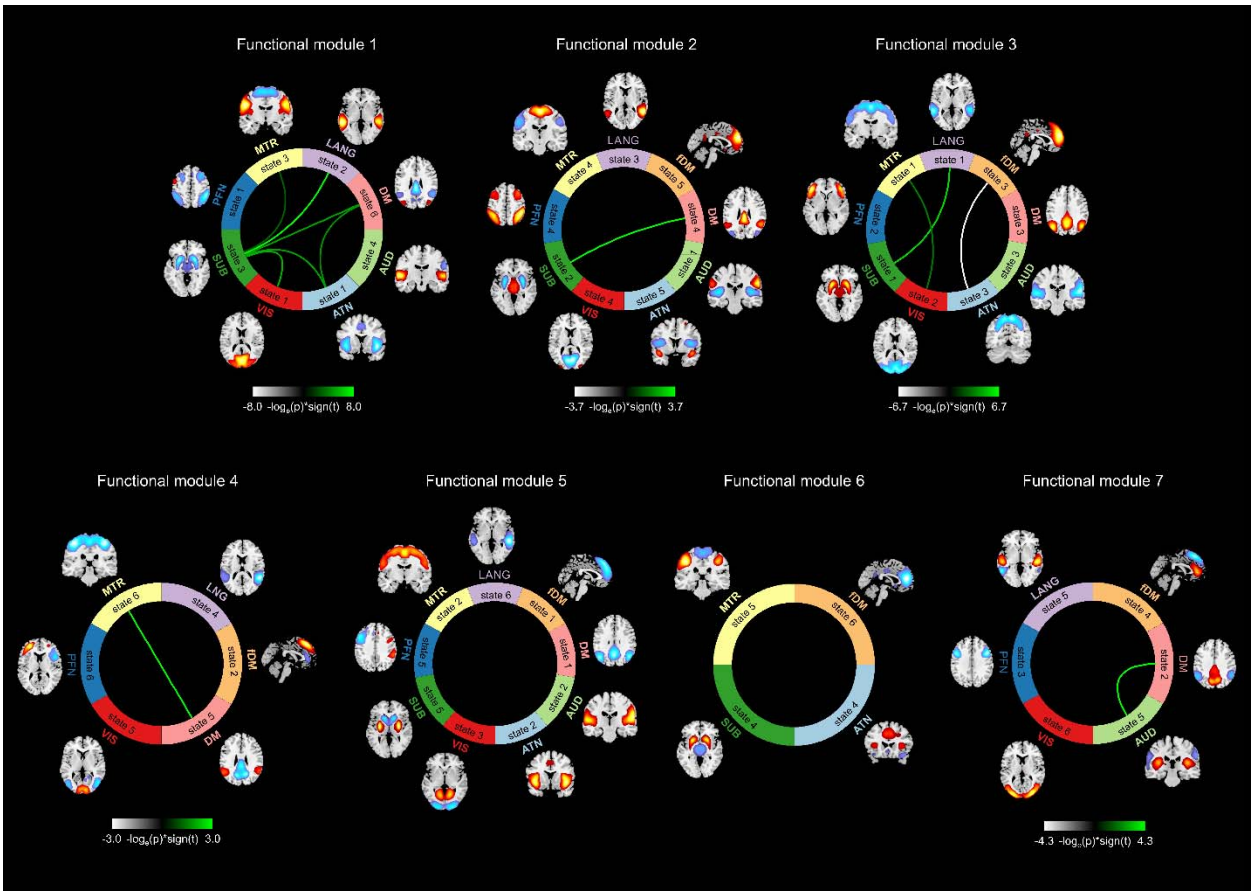

Figure 8. Functional modules and functional state connectivity comparisons between healthy subjects and patients with schizophrenia (SZ). Seven functional modules were detected using Newman modularity detection approach. The green lines represent higher functional state connectivity in healthy subjects than SZ patients, and the silver one shows a higher functional state connectivity in SZ patients.

Discussion

The brain reorganizes itself on different temporal and spatial scales which manifest at the macro level as variations in the temporal and also spatial couplings of brain functional organization. The majority of studies have focused on temporal coupling and overlooked spatial coupling. In the present study, we probed the spatiotemporal variations of the functional domains and show that functional domains are evolving spatially over time. Motivated by this discovery, we used clustering to summarize the activity patterns of the functional domains. This resulted in a set of distinct and reproducible spatial patterns called spatial domain states and allowed us to further examine the time-varying properties of functional domains. Variations of functional domains over time further buttress by changes in a region's

membership across states which can explain the inconsistency in regions' memberships to functional domains reflected across previous findings. Alternative interpretations for the observed inconsistency in the spatial patterns of functional domains may be drawn by examining findings from studies of individual variability across resting state and fluctuations during task (Braga and Buckner, 2017; Cole et al., 2013). We proposed that the temporal variations of spatial coupling are another reason for the variability in regions' memberships and confirmed our findings by investigating the amplitude of BOLD signal. We observed a direct relationship between the activities of regions measured by the BOLD signal and their contributions to functional domains which supports our proposition that regions have higher/lower activity than their baseline when they have positive/negative association to their corresponding functional domains. Another explanation for such variations can be parallel interdigitated distributed networks detected in subject-level analysis (Braga and Buckner, 2017). Their findings suggests that each functional domain may consist of parallel networks that work simultaneously and only one of them is captured in group-level analysis. The concept of the temporal variations of spatial coupling is not opposing the idea of parallel processing within functional domains, as they can also be captured via brain dynamic analysis using our approach. Because a brain region's association to functional domains can vary over the time, the parallel networks can be captured using the time points that they are the dominant patterns within their corresponding functional domains. Similar differences in regional associations reported across parallel networks in subject-level analysis (Braga and Buckner, 2017) were also observed across the states of functional domains in this study.

Approach and its strengths: Our proposed approach is based on the well-accepted assumption that the brain can be modelled as a hierarchical functional architecture with different levels of granularity. Each level of this architecture includes several elements that each element involves in specific functions, and as we move to the higher levels of this architecture, the number of functions associated with elements increases. In other words, the elements of higher levels have less functional homogeneity and increased dynamic behavior. Studying this architecture at a macro-scale, there is a level that its elements can be

approximated as functional units. A functional unit is a pattern of regions with the same functional activity over time. Our approach approximates functional units as hICNs obtained from high-order ICA and reconstructs functional domains using both spatial and temporal information of hICNs. Here, estimation of functional units and spatially fluid properties are limited by the spatial/temporal resolutions and the properties of the imaging modality. We can improve the functional granularity and reconstruct the hierarchy from lower levels, such as cortical columns, by adjusting the data acquisition and analytical approaches. The approach can also be applied on other imaging modalities, such as calcium imaging (Matsui et al., 2018) or photoacoustic tomography (Nasiriavanaki et al., 2014), to provide better understanding of the spatially fluid properties and information processing across this hierarchy. Employing both spatial and temporal information of ICNs is another advantage of this work. The approach provides information of each functional domain at every timepoint and has the capacity to examine spatiotemporal variations of the functional domains up to the maximum temporal and spatial resolutions exist in the data. Although one main advantages of this work is its ability to investigate dynamic behavior within each functional domain, it also allows us to look at changes in the relationship among functional domains. For this purpose, we introduced a technique to access the relationship between functional domains and capture the connectivity patterns (i.e. functional modules) among them. The approach provides us a new set of measurements and metrics of brain function, and our preliminary analysis on patients with schizophrenia indicate that the approach can be a promising tool for basic neuroscience and clinical investigations.

Schizophrenia: Schizophrenia (SZ) is a heterogeneous disorder characterized by symptoms of impaired reality testing such as hallucinations, delusions, and frequently disorganized speech and behavior, as well as impairments in cognition across a range of domains. It has been suggested that schizophrenia is related to the brain's reduced capacity to integrate information across the different regions (Kahn et al., 2015; Stephan et al., 2006). Patients with schizophrenia show lower global functional connectivity between many regions, including: subcortical regions, the frontal, temporal, and occipital cortices. A replicated

exception to this trend is increased functional connectivity between the thalamus and somatosensory and motor areas (Argyelan et al., 2014; Damaraju et al., 2014; Giraldo-Chica and Woodward, 2017; Skudlarski et al., 2010; Tu et al., 2015). The "Disconnection hypothesis" (i.e. dysconnectivity) of schizophrenia introduced by Friston, 1998, suggests that impaired synaptic plasticity is the source of abnormal functional integration (functional dysconnectivity) of neural systems (Friston, 1998). Alternatively, reduced functional connectivity among brain regions might be due to alterations in structural connections within the brain, which is also commonly reported among SZ patients (Kahn et al., 2015). Using "graph theory", van den Heuvel et al. found that brain structural connections of SZ patients have lower capacity to integrate information across brain regions (van den Heuvel et al., 2010). These two mechanisms, dysconnectivity and abnormal structural connections, can coexist (Kahn et al., 2015). Changes across whole brain are not limited to brain connectivity. Reductions in grey and white matter volumes and gray matter deficits have been reported across whole brain including thalamus, frontal, temporal, cingulate and insular cortex (Ellison-Wright and Bullmore, 2010; Kahn et al., 2015; Segall et al., 2009; Staal et al., 2001). Our findings shed new light on these phenomenon of decreasing patterns, highlighting a global reduction in brain functional activity within specific functional domains. Furthermore, functional state connectivity within functional modules is in agreement with the hypoconnectivity observed in previous studies among brain regions. Interestingly, unlike the constant general pattern of hypoconnectivity, increased functional connectivity between subcortical and sensorimotor regions have been previously reported (Argyelan et al., 2014; Giraldo-Chica and Woodward, 2017). While we did not investigate functional connectivity between brain regions, we observed decreased functional state connectivity between subcortical and somatosensory and motor domains within the functional modules, which could be an important window into a link between increased functional connectivity among these regions and decreased functional connectivity with the rest of the brain.

In our analysis, the most affected regions and domains include the thalamus of the subcortical domain; BA 38 of the attention domain; the left insula, the left BA 44, the right BA 41/42 and the rostral area of left BA 22 of the language domain; and the fusiform gyrus and the medioventral and lateral occipital cortex of the visual domain. There is considerable evidence that most of these regions are abnormal in schizophrenia. The thalamus is known as a major brain structure affected both structurally and functionally in SZ patients (Cheng et al., 2015; Damaraju et al., 2014; Giraldo-Chica and Woodward, 2017). Schizophrenia is a cognitive and behavioral disorder including disruption in attention associated areas (Bowie and Harvey, 2006). Temporal pole area BA38 is a key part of the theory of mind (ToM) network, that is classically impaired in individuals with schizophrenia and autism-spectrum disorder (Assaf et al., 2010). Furthermore, BA 41/42 is primary auditory cortex, and together with the BA22 (Auditory association cortex/Wernicke's area), has been repeatedly implicated in the pathophysiology of auditory hallucinations in schizophrenia (Barta et al., 1990; Gavrilescu et al., 2010; Shinn et al., 2013; Vercammen et al., 2010). Alterations in the visual domain have been also observed as ocular convergence deficits (Bolding et al., 2012) and reduce amplitude of low-frequency fluctuations (ALFF) was observed across visual areas including the cuneus and lingual gyrus (Hoptman et al., 2010).

Limitations and future directions: The proposed approach, in a nutshell, reconstructs each functional domain from its pieces to capture the dynamic properties of the functional domain. Although any partitioning of functional domains expresses similar findings, a good partitioning is essential to fully capture the dynamic characteristics of the data. An assumption behind the proposed approach is that hICNs are a good approximation of functional units that can be obtained from fMRI data. While using hICNs has advantages over predefined anatomical regions as they contains functionally homogeneous regions obtained from data itself, the level of parcellation (i.e. a number of components) is important and needs further investigation. In addition to the number of hICNs, changes in hICNs' memberships to functional domains over time is another crucial factor that needs to be considered. The present study limits assigning each hICN to one functional domain based on the prior knowledge and the dominant

functional properties; however, hICNs can also change their memberships to functional domains over time. Ongoing work is assigning hICNs to functional domains at any given timepoint using the information of the data in that timepoint. Characterizing the dynamic behavior of functional domains is another area that needs further investigation. This study was directed to demonstrate variations in the spatial couplings of functional domains over time and used k-means clustering to define a set of representatives. Measures such as dwell time, leave time, and transition are some examples that can be used to evaluate the dynamic characteristics within and between functional domains. It is apropos to mention that, in this study, k-means clustering was merely used as a tool to examine variations existing in brain functional domains. While it yields valuable results, neither the states identified using k-means clustering are likely to be the true origins of time-varying behavior of functional domains nor activity patterns of functional domains cannot occur simultaneously. Further studies are therefore needed to find improved representations of the time-varying behavior of functional domains.

Conclusion

The present work reveals evidence of variations in the spatial coupling of functional domains over time. The proposed approach provides a new framework to study brain function and evaluate the spatiotemporal variations of brain functional domains. Preliminary assessments of the approach using healthy controls and patients with schizophrenia demonstrate the ability of the approach to obtain new information of the brain function and detect alterations among SZ patients. However, further investigations using different datasets and various groups of cohorts should be performed to evaluate the benefits of studying spatiotemporal variations of brain functional domains for both basic and clinical neuroscience applications.

Acknowledgments

This work was supported by grants from the National Institutes of Health grant numbers 2R01EB005846, R01REB020407, and P20GM103472; and National Science Foundation (NSF) grant 1539067 to Dr.

Vince Calhoun. We thank Srinivas Rachakonda, Dr. Thomas P. DeRamus, Dr. Maziar Yaesoubi, Dr. Rhoshel K Lenroot, and Dr. Juan R. Bustillo for their input.

References

Allen, E.A., Damaraju, E., Plis, S.M., Erhardt, E.B., Eichele, T., Calhoun, V.D., 2014. Tracking whole-brain connectivity dynamics in the resting state. Cereb Cortex 24, 663-676.

Allen, E.A., Erhardt, E.B., Damaraju, E., Gruner, W., Segall, J.M., Silva, R.F., Havlicek, M., Rachakonda, S., Fries, J., Kalyanam, R., Michael, A.M., Caprihan, A., Turner, J.A., Eichele, T., Adelsheim, S., Bryan, A.D., Bustillo, J., Clark, V.P., Feldstein Ewing, S.W., Filbey, F., Ford, C.C., Hutchison, K., Jung, R.E., Kiehl, K.A., Kodituwakku, P., Komesu, Y.M., Mayer, A.R., Pearlson, G.D., Phillips, J.P., Sadek, J.R., Stevens, M., Teuscher, U., Thoma, R.J., Calhoun, V.D., 2011. A baseline for the multivariate comparison of resting-state networks. Front Syst Neurosci 5, 2.

Arbabshirani, M.R., Plis, S., Sui, J., Calhoun, V.D., 2017. Single subject prediction of brain disorders in neuroimaging: Promises and pitfalls. Neuroimage 145, 137-165.

Argyelan, M., Ikuta, T., DeRosse, P., Braga, R.J., Burdick, K.E., John, M., Kingsley, P.B., Malhotra, A.K., Szeszko, P.R., 2014. Resting-state fMRI connectivity impairment in schizophrenia and bipolar disorder. Schizophr Bull 40, 100-110.

Assaf, M., Jagannathan, K., Calhoun, V.D., Miller, L., Stevens, M.C., Sahl, R., O'Boyle, J.G., Schultz, R.T., Pearlson, G.D., 2010. Abnormal functional connectivity of default mode sub-networks in autism spectrum disorder patients. Neuroimage 53, 247-256.

Barta, P.E., Pearlson, G.D., Powers, R.E., Richards, S.S., Tune, L.E., 1990. Auditory hallucinations and smaller superior temporal gyral volume in schizophrenia. Am J Psychiatry 147, 1457-1462.

Benjamini, Y., Hochberg, Y., 1995. Controlling the False Discovery Rate: A Practical and Powerful Approach to Multiple Testing. Journal of the Royal Statistical Society. Series B (Methodological) 57, 289-300.

Biswal, B.B., Mennes, M., Zuo, X.N., Gohel, S., Kelly, C., Smith, S.M., Beckmann, C.F., Adelstein, J.S., Buckner, R.L., Colcombe, S., Dogonowski, A.M., Ernst, M., Fair, D., Hampson, M., Hoptman, M.J., Hyde, J.S., Kiviniemi, V.J., Kotter, R., Li, S.J., Lin, C.P., Lowe, M.J., Mackay, C., Madden, D.J., Madsen, K.H., Margulies, D.S., Mayberg, H.S., McMahon, K., Monk, C.S., Mostofsky, S.H., Nagel, B.J., Pekar, J.J., Peltier, S.J., Petersen, S.E., Riedl, V., Rombouts, S.A., Rypma, B., Schlaggar, B.L., Schmidt, S., Seidler, R.D., Siegle, G.J., Sorg, C., Teng, G.J., Veijola, J., Villringer, A., Walter, M., Wang, L., Weng, X.C., Whitfield-Gabrieli, S., Williamson, P., Windischberger, C., Zang, Y.F., Zhang, H.Y., Castellanos, F.X., Milham, M.P., 2010. Toward discovery science of human brain function. Proc Natl Acad Sci U S A 107, 4734-4739.

Bolding, M.S., Lahti, A.C., Gawne, T.J., Hopkins, K.B., Gurler, D., Gamlin, P.D., 2012. Ocular Convergence Deficits in Schizophrenia. Front Psychiatry 3.

Bowie, C.R., Harvey, P.D., 2006. Cognitive deficits and functional outcome in schizophrenia. Neuropsychiatr Dis Treat 2, 531-536.

Braga, R.M., Buckner, R.L., 2017. Parallel Interdigitated Distributed Networks within the Individual Estimated by Intrinsic Functional Connectivity. Neuron 95, 457-471 e455.

Buckner, R.L., Sepulcre, J., Talukdar, T., Krienen, F.M., Liu, H., Hedden, T., Andrews-Hanna, J.R., Sperling, R.A., Johnson, K.A., 2009. Cortical hubs revealed by intrinsic functional connectivity: mapping, assessment of stability, and relation to Alzheimer's disease. J Neurosci 29, 1860-1873.

Calhoun, V., Adali, T., 2002. Complex infomax: Convergence and approximation of infomax with complex nonlinearities. Neural Networks for Signal Processing Xii, Proceedings, 307-316.

Calhoun, V.D., Adali, T., 2012. Multisubject independent component analysis of fMRI: a decade of intrinsic networks, default mode, and neurodiagnostic discovery. IEEE Rev Biomed Eng 5, 60-73.

Calhoun, V.D., Adali, T., Pearlson, G.D., Pekar, J.J., 2001. A method for making group inferences from functional MRI data using independent component analysis. Hum Brain Mapp 14, 140-151.

Calhoun, V.D., de Lacy, N., 2017. Ten Key Observations on the Analysis of Resting-state Functional MR Imaging Data Using Independent Component Analysis. Neuroimaging Clin N Am 27, 561-579.

Calhoun, V.D., Kiehl, K.A., Pearlson, G.D., 2008. Modulation of temporally coherent brain networks estimated using ICA at rest and during cognitive tasks. Hum Brain Mapp 29, 828-838.

Calhoun, V.D., Liu, J., Adali, T., 2009. A review of group ICA for fMRI data and ICA for joint inference of imaging, genetic, and ERP data. Neuroimage 45, S163-172.

Calhoun, V.D., Miller, R., Pearlson, G., Adali, T., 2014. The chronnectome: time-varying connectivity networks as the next frontier in fMRI data discovery. Neuron 84, 262-274.

Cheng, W., Palaniyappan, L., Li, M., Kendrick, K.M., Zhang, J., Luo, Q., Liu, Z., Yu, R., Deng, W., Wang, Q., Ma, X., Guo, W., Francis, S., Liddle, P., Mayer, A.R., Schumann, G., Li, T., Feng, J., 2015. Voxel-based, brain-wide association study of aberrant functional connectivity in schizophrenia implicates thalamocortical circuitry. NPJ Schizophr 1, 15016.

Cole, M.W., Reynolds, J.R., Power, J.D., Repovs, G., Anticevic, A., Braver, T.S., 2013. Multi-task connectivity reveals flexible hubs for adaptive task control. Nat Neurosci 16, 1348-1355.

Correa, N., Adali, T., Calhoun, V.D., 2007. Performance of blind source separation algorithms for fMRI analysis using a group ICA method. Magn Reson Imaging 25, 684-694.

Correa, N., Adali, T., Yi-Ou, L., Calhoun, V.D., 2005. Comparison of blind source separation algorithms for FMRI using a new Matlab toolbox: GIFT. Acoustics, Speech, and Signal Processing, 2005. Proceedings. (ICASSP '05). IEEE International Conference on, pp. v/401-v/404 Vol. 405.

Damaraju, E., Allen, E.A., Belger, A., Ford, J.M., McEwen, S., Mathalon, D.H., Mueller, B.A., Pearlson, G.D., Potkin, S.G., Preda, A., Turner, J.A., Vaidya, J.G., van Erp, T.G., Calhoun, V.D., 2014. Dynamic functional connectivity analysis reveals transient states of dysconnectivity in schizophrenia. Neuroimage Clin 5, 298-308.

Dice, L.R., 1945. Measures of the Amount of Ecologic Association between Species. Ecology 26, 297-302.

Du, W., Ma, S., Fu, G.S., Calhoun, V.D., Adalı, T., 2014. A novel approach for assessing reliability of ICA for FMRI analysis. 2014 IEEE International Conference on Acoustics, Speech and Signal Processing (ICASSP), pp. 2084-2088.

Ellison-Wright, I., Bullmore, E., 2010. Anatomy of bipolar disorder and schizophrenia: a meta-analysis. Schizophr Res 117, 1-12.

Erhardt, E.B., Allen, E.A., Damaraju, E., Calhoun, V.D., 2011. On network derivation, classification, and visualization: a response to Habeck and Moeller. Brain Connect 1, 1-19.

Fan, L., Li, H., Zhuo, J., Zhang, Y., Wang, J., Chen, L., Yang, Z., Chu, C., Xie, S., Laird, A.R., Fox, P.T., Eickhoff, S.B., Yu, C., Jiang, T., 2016. The Human Brainnetome Atlas: A New Brain Atlas Based on Connectional Architecture. Cereb Cortex 26, 3508-3526.

Franco, A.R., Pritchard, A., Calhoun, V.D., Mayer, A.R., 2009. Interrater and Intermethod Reliability of Default Mode Network Selection. Hum Brain Mapp 30, 2293-2303.

Friston, K.J., 1998. The disconnection hypothesis. Schizophr Res 30, 115-125.

Friston, K.J., Frith, C.D., Liddle, P.F., Frackowiak, R.S., 1993. Functional connectivity: the principal-component analysis of large (PET) data sets. J Cereb Blood Flow Metab 13, 5-14.

Garrity, A.G., Pearlson, G.D., McKiernan, K., Lloyd, D., Kiehl, K.A., Calhoun, V.D., 2007. Aberrant "default mode" functional connectivity in schizophrenia. Am J Psychiatry 164, 450-457.

Gavrilescu, M., Rossell, S., Stuart, G.W., Shea, T.L., Innes-Brown, H., Henshall, K., McKay, C., Sergejew, A.A., Copolov, D., Egan, G.F., 2010. Reduced connectivity of the auditory cortex in patients with auditory hallucinations: a resting state functional magnetic resonance imaging study. Psychol Med 40, 1149-1158.

Giraldo-Chica, M., Woodward, N.D., 2017. Review of thalamocortical resting-state fMRI studies in schizophrenia. Schizophr Res 180, 58-63.

Greicius, M., 2008. Resting-state functional connectivity in neuropsychiatric disorders. Curr Opin Neurol 21, 424-430.

Guo, C.C., Kurth, F., Zhou, J., Mayer, E.A., Eickhoff, S.B., Kramer, J.H., Seeley, W.W., 2012. One-year test-retest reliability of intrinsic connectivity network fMRI in older adults. Neuroimage 61, 1471-1483.

Himberg, J., Hyvarinen, A., Esposito, F., 2004. Validating the independent components of neuroimaging time series via clustering and visualization. Neuroimage 22, 1214-1222.

Hoaglin, D.C., Iglewicz, B., Tukey, J.W., 1986. Performance of Some Resistant Rules for Outlier Labeling. Journal of the American Statistical Association 81, 991-999.

Hoptman, M.J., Zuo, X.N., Butler, P.D., Javitt, D.C., D'Angelo, D., Mauro, C.J., Milham, M.P., 2010. Amplitude of low-frequency oscillations in schizophrenia: a resting state fMRI study. Schizophr Res 117, 13-20.

Hutchison, R.M., Womelsdorf, T., Allen, E.A., Bandettini, P.A., Calhoun, V.D., Corbetta, M., Della Penna, S., Duyn, J.H., Glover, G.H., Gonzalez-Castillo, J., Handwerker, D.A., Keilholz, S., Kiviniemi,

V., Leopold, D.A., de Pasquale, F., Sporns, O., Walter, M., Chang, C., 2013. Dynamic functional connectivity: promise, issues, and interpretations. Neuroimage 80, 360-378.

Kahn, R.S., Sommer, I.E., Murray, R.M., Meyer-Lindenberg, A., Weinberger, D.R., Cannon, T.D., O'Donovan, M., Correll, C.U., Kane, J.M., van Os, J., Insel, T.R., 2015. Schizophrenia. Nature Reviews Disease Primers 1, 15067.

Kiviniemi, V., Vire, T., Remes, J., Elseoud, A.A., Starck, T., Tervonen, O., Nikkinen, J., 2011. A sliding time-window ICA reveals spatial variability of the default mode network in time. Brain Connect 1, 339-347.

Lin, Q.H., Liu, J., Zheng, Y.R., Liang, H., Calhoun, V.D., 2010. Semiblind spatial ICA of fMRI using spatial constraints. Hum Brain Mapp 31, 1076-1088.

Ma, S., Calhoun, V.D., Phlypo, R., Adali, T., 2014. Dynamic changes of spatial functional network connectivity in healthy individuals and schizophrenia patients using independent vector analysis. Neuroimage 90, 196-206.

Ma, S., Correa, N.M., Li, X.-L., Eichele, T., Calhoun, V.D., Adalı, T., 2011. Automatic Identification of Functional Clusters in fMRI Data using Spatial Information. IEEE transactions on bio-medical engineering 58, 3406-3417.

Matsui, T., Murakami, T., Ohki, K., 2018. Neuronal Origin of the Temporal Dynamics of Spontaneous BOLD Activity Correlation. Cereb Cortex.

Menon, V., 2011. Large-scale brain networks and psychopathology: a unifying triple network model. Trends Cogn Sci 15, 483-506.

Nasiriavanaki, M., Xia, J., Wan, H., Bauer, A.Q., Culver, J.P., Wang, L.V., 2014. High-resolution photoacoustic tomography of resting-state functional connectivity in the mouse brain. Proc Natl Acad Sci U S A 111, 21-26.

Newman, M.E., 2006. Modularity and community structure in networks. Proc Natl Acad Sci U S A 103, 8577-8582.

Petersen, S.E., Sporns, O., 2015. Brain Networks and Cognitive Architectures. Neuron 88, 207-219.

Power, J.D., Barnes, K.A., Snyder, A.Z., Schlaggar, B.L., Petersen, S.E., 2012. Spurious but systematic correlations in functional connectivity MRI networks arise from subject motion. Neuroimage 59, 2142-2154.

Preti, M.G., Bolton, T.A., Van De Ville, D., 2017. The dynamic functional connectome: State-of-the-art and perspectives. Neuroimage 160, 41-54.

Sakoglu, U., Pearlson, G.D., Kiehl, K.A., Wang, Y.M., Michael, A.M., Calhoun, V.D., 2010. A method for evaluating dynamic functional network connectivity and task-modulation: application to schizophrenia. MAGMA 23, 351-366.

Seeley, W.W., Crawford, R.K., Zhou, J., Miller, B.L., Greicius, M.D., 2009. Neurodegenerative diseases target large-scale human brain networks. Neuron 62, 42-52.

Segall, J.M., Turner, J.A., van Erp, T.G., White, T., Bockholt, H.J., Gollub, R.L., Ho, B.C., Magnotta, V., Jung, R.E., McCarley, R.W., Schulz, S.C., Lauriello, J., Clark, V.P., Voyvodic, J.T., Diaz, M.T., Calhoun, V.D., 2009. Voxel-based morphometric multisite collaborative study on schizophrenia. Schizophr Bull 35, 82-95.

Shehzad, Z., Kelly, A.M., Reiss, P.T., Gee, D.G., Gotimer, K., Uddin, L.Q., Lee, S.H., Margulies, D.S., Roy, A.K., Biswal, B.B., Petkova, E., Castellanos, F.X., Milham, M.P., 2009. The resting brain: unconstrained yet reliable. Cereb Cortex 19, 2209-2229.

Shinn, A.K., Baker, J.T., Cohen, B.M., Ongur, D., 2013. Functional connectivity of left Heschl's gyrus in vulnerability to auditory hallucinations in schizophrenia. Schizophr Res 143, 260-268.

Skudlarski, P., Jagannathan, K., Anderson, K., Stevens, M.C., Calhoun, V.D., Skudlarska, B.A., Pearlson, G., 2010. Brain connectivity is not only lower but different in schizophrenia: a combined anatomical and functional approach. Biol Psychiatry 68, 61-69.

Smith, S.M., Fox, P.T., Miller, K.L., Glahn, D.C., Fox, P.M., Mackay, C.E., Filippini, N., Watkins, K.E., Toro, R., Laird, A.R., Beckmann, C.F., 2009. Correspondence of the brain's functional architecture during activation and rest. Proc Natl Acad Sci U S A 106, 13040-13045.

Sorg, C., Riedl, V., Muhlau, M., Calhoun, V.D., Eichele, T., Laer, L., Drzezga, A., Forstl, H., Kurz, A., Zimmer, C., Wohlschlager, A.M., 2007. Selective changes of resting-state networks in individuals at risk for Alzheimer's disease. Proc Natl Acad Sci U S A 104, 18760-18765.

Staal, W.G., Hulshoff Pol, H.E., Schnack, H.G., van Haren, N.E., Seifert, N., Kahn, R.S., 2001. Structural brain abnormalities in chronic schizophrenia at the extremes of the outcome spectrum. Am J Psychiatry 158, 1140-1142.

Stephan, K.E., Baldeweg, T., Friston, K.J., 2006. Synaptic plasticity and dysconnection in schizophrenia. Biol Psychiatry 59, 929-939.

Trapp, C., Vakamudi, K., Posse, S., 2018. On the detection of high frequency correlations in resting state fMRI. Neuroimage 164, 202-213.

Tu, P.C., Lee, Y.C., Chen, Y.S., Hsu, J.W., Li, C.T., Su, T.P., 2015. Network-specific cortico-thalamic dysconnection in schizophrenia revealed by intrinsic functional connectivity analyses. Schizophr Res 166, 137-143.

van den Heuvel, M.P., Hulshoff Pol, H.E., 2010. Exploring the brain network: a review on resting-state fMRI functional connectivity. Eur Neuropsychopharmacol 20, 519-534.

van den Heuvel, M.P., Mandl, R.C., Kahn, R.S., Hulshoff Pol, H.E., 2009. Functionally linked resting-state networks reflect the underlying structural connectivity architecture of the human brain. Hum Brain Mapp 30, 3127-3141.

van den Heuvel, M.P., Mandl, R.C., Stam, C.J., Kahn, R.S., Hulshoff Pol, H.E., 2010. Aberrant frontal and temporal complex network structure in schizophrenia: a graph theoretical analysis. J Neurosci 30, 15915-15926.

Van Dijk, K.R., Hedden, T., Venkataraman, A., Evans, K.C., Lazar, S.W., Buckner, R.L., 2010. Intrinsic functional connectivity as a tool for human connectomics: theory, properties, and optimization. J Neurophysiol 103, 297-321.

Vercammen, A., Knegtering, H., den Boer, J.A., Liemburg, E.J., Aleman, A., 2010. Auditory hallucinations in schizophrenia are associated with reduced functional connectivity of the temporo-parietal area. Biol Psychiatry 67, 912-918.

Vidaurre, D., Smith, S.M., Woolrich, M.W., 2017. Brain network dynamics are hierarchically organized in time. Proc Natl Acad Sci U S A 114, 12827-12832.

Yaesoubi, M., Adali, T., Calhoun, V.D., 2018. A window-less approach for capturing time-varying connectivity in fMRI data reveals the presence of states with variable rates of change. Hum Brain Mapp 39, 1626-1636.

Yaesoubi, M., Miller, R.L., Calhoun, V.D., 2017. Time-varying spectral power of resting-state fMRI networks reveal cross-frequency dependence in dynamic connectivity. PLoS One 12, e0171647.

Yarkoni, T., Poldrack, R.A., Nichols, T.E., Van Essen, D.C., Wager, T.D., 2011. Large-scale automated synthesis of human functional neuroimaging data. Nat Methods 8, 665-670.

Yeo, B.T., Krienen, F.M., Sepulcre, J., Sabuncu, M.R., Lashkari, D., Hollinshead, M., Roffman, J.L., Smoller, J.W., Zollei, L., Polimeni, J.R., Fischl, B., Liu, H., Buckner, R.L., 2011. The organization of the human cerebral cortex estimated by intrinsic functional connectivity. J Neurophysiol 106, 1125-1165.

Zuo, X.N., Kelly, C., Adelstein, J.S., Klein, D.F., Castellanos, F.X., Milham, M.P., 2010. Reliable intrinsic connectivity networks: test-retest evaluation using ICA and dual regression approach. Neuroimage 49, 2163-2177.